RTS/03-01SDR/SwRI

A Preliminary Numerical Study of the Hazard from Local Landslide Tsunami Scenarios at the Diablo Canyon Site in Central California

Summary Report (Draft)
November 22, 2003

Investigator:

Dr. R.T. Sewell
R.T. Sewell Associates, Consulting
Louisville, Colorado

Prepared for:

Southwest Research Institute
U.S. Nuclear Regulatory Commission

Table of Contents

List of Tables

List of Figures

List of Figures (continued)

1. Background and Introduction

The safety analysis report (SAR) for the Diablo Canyon Independent Spent Fuel Storage Installation (DC-ISFSI) references the tsunami design basis (and related tsunami studies) cited in the final safety analysis report (FSAR) for the Diablo Canyon Power Plant (DCPP). With respect to tsunamis, the DCPP FSAR indicates that a maximum combined wave run-up of 34.6 ft [+10.5 m] (relative to the mean lower low water [MLLW] level[1]), and maximum combined wave draw-down of 9.0 ft [-2.7 m] MLLW, were developed as the design basis. Those values were determined based on a deterministic probable maximum tsunami analysis that considered enveloping effects of both potential distantly generated tsunamis and potential locally generated tsunamis.

The predominant sources of distantly generated tsunamis were taken to be areas of earthquake and volcanic activity on the circum-Pacific belt. The historical case of 17 to 20 ft waves being experienced at Crescent City, California as a result of the 1964 Anchorage, Alaska earthquake was used as justification for deciding that a maximum wave run-up of 20 ft would have "virtually no risk of being exceeded" at the Diablo Canyon site. When combined with other wave effects (tide, storm surge, wind-induced waves), a maximum combined wave run-up of 30 ft [9.1 m] was developed for distantly generated tsunamis. For locally generated tsunamis, two hypothetical offshore earthquake scenarios were considered: (1) an event on the Santa Lucia Bank Fault having a resultant co-seismic displacement of 9.8 ft [3.0 m] with vertical component equal to 6.6 ft [2.0 m]; and (2) an event on the Santa Maria Basin Fault (Hosgri Fault) having a resultant co-seismic displacement of 11 ft [3.4 m] with vertical component equal to 7.3 ft [2.2 m]. Analyses of these events in 1975 by Hwang et al. indicated that the latter event would produce the controlling effect among the two local scenarios, with a peak wave run-up of 9.2 ft [2.8 m]. Ultimately, however, the results of scale model tests (that were performed after a severe storm occurred at the Diablo Canyon site during January 1981) were used to develop a combined wave run-up of 34.6 ft [10.5 m] for locally generated tsunamis.

The judgments and analyses used to develop the DCPP tsunami design basis were representative of the contemporary approaches, information, and expertise then available. Nearly three decades have past since the time that the design tsunami scenarios for DCPP were developed and analyzed. Since then, significant advancements have taken place in the field of tsunami science, and those advances affect both the selection and analysis of scenarios used for tsunami hazard

[1] At the Diablo Canyon site, MLLW is 2.6 feet [0.79 m] below mean sea level (MSL).

assessment. One such advancement is the greater experience and realization regarding the significance (in terms of both likelihood and potential effects) of landslide tsunamis. Another advancement has been in the area of characterization and numerical modeling of tsunamis. Aside from these advancements in tsunami science, there have simultaneously occurred advances in general methods of hazard and risk assessment, evaluation of expert uncertainties, and their integration into performance-based and risk-informed decision making. In modern application, probabilistic methods are typically being applied for hazard and risk assessment and for regulatory use of such assessments. Correspondingly, more consistent consideration is being given to the time frame – including scenario repeat times (i.e., recurrence intervals) and repeat times of their site effects (i.e., return periods) – of design and/or potential failure events.

These observations suggest that the DCPP tsunami hazard assessment may need to be updated to reflect modern scientific understanding and analysis methods, as well as modern application of hazard/risk assessment (including evaluation of uncertainties). An update is warranted primarily if the use of modern approaches and evidence suggests that the existing tsunami design basis is likely to be non-conservative and the tsunami risk is likely to be significantly higher than originally thought. Correspondingly, the purpose of the present study is to identify and analyze tsunami scenarios based on current scientific understanding and considerations, and evaluate whether or not the existing bases for tsunami design at the Diablo Canyon site (for DCPP and DC-ISFSI) still appear adequate.

2. Scope of this Study

In terms of identification of tsunami scenarios, perhaps the most relevant consideration for the present study is that of landslide tsunamis. Such scenarios were not explicitly considered in the development of the DCPP tsunami design basis. They may be triggered by various events including earthquakes, gas hydrate releases, wave action, explosions, static overload, or a combination of effects. The available evidence suggests that such scenarios are likely to be an important contributor to the overall tsunami hazard at many coastal locations. This evidence encompasses the possibility of both distantly generated and locally generated landslide tsunamis. In terms of distantly generated events, there are, for instance, the cases of volcanic flank collapses (such as those a number of scientific studies suggest have occurred in the geological past along the Hawaiian volcanic chain [in the Pacific] and the Canary Islands [in the Atlantic] and likely produced large local and distant tsunamis). In terms of locally generated events, there is the recent case of the 1998 Papua New Guinea tsunami that produced a maximum local run-up of about 50 ft [15 m] (and which the latest evidence suggests resulted in large part from a local submarine landslide that was triggered by the seismic event). Other historical cases of submarine landslides are associated with estimated maximum local wave run-up of about 105 meters [344 ft] (1946 Aleutian earthquake in the vicinity of Scotch Cap), whereas historical sub-aerial slides have produced measured local wave run-up exceeding 1,719 m [1,640 ft] (Lituya Bay, Alaska tsunami of July 9, 1958). (The latter event, however, is not considered to be representative of local conditions that are likely to produce the dominant tsunami effect at the Diablo Canyon site.)

Information submitted with the DC-ISFSI SAR (PG&E, 2002) provides qualitative discussion and judgments that were used to essentially screen out landslide tsunamis from more detailed consideration. In several respects (e.g., see Sewell, 2002), those qualitative judgments do not appear to adequately reflect the available data, scientific understanding, and time frames that need to be considered for safety analysis and design of a critical facility[2]. This is particularly the case for potential local submarine landslide events. As one example, the SAR gave no consideration to the potential and effects of submarine landslides north of San Simeon and south of Pt. Arguello (see Figure 1), whereas deep canyons offshore Monterey / Carmel and steep escarpments offshore of Pt. Sur (to the north of San Simeon) as well as slopes within and near the mouth of Santa Barbara Channel are known to be capable of producing tsunamigenic submarine landslides (such as the historical 150 km^2 submarine landslide on December 21, 1812 that produced estimated wave amplitudes of about 10 m [33 ft] at Goleta, California). As another example, the SAR states that the average slope of the continental shelf is nearly flat, being about 1 degree; and the continental slope has a shallow slope that averages 6 degrees. However, the SAR does not note the fact that submarine slides are common on gentle slopes, and does not note the areas of maximum slope (as opposed to average slope) where the potential for sliding is greater. Significant slides on slopes of less than 3 percent, or 1.7 degrees, are not uncommon. Additionally, with respect to the Diablo Canyon site, there are several areas along the near-offshore continental shelf having slopes in excess of 1 degree, and many areas along the near-offshore continental slope having slopes in excess of 6 degrees (the area of Santa Lucia Escarpment, as one example, has slopes up to about 40 percent, or 22 degrees).

---

[2] In addition to the precedents in nuclear safety management, another example of design-basis for a critical facility is the case of liquefied natural gas (LNG) plants, where design standards (NFPA 59A) specify a return period of at least 475 years for the operating basis earthquake (OBE) and 10,000 years for the safe shutdown earthquake (SSE).

There exists a comparatively larger body of detailed information pertaining to submarine features, geology, and potential slide areas offshore north-central and southern California, as compared to the information available for the area of offshore south-central California near the Diablo Canyon site. This situation is likely owing to the relatively lower population density along coastal south-central California (e.g., between Monterey and Santa Barbara). However, examination of the literature pertaining to known slides immediately surrounding this area, and examination of the available bathymetry for this area, suggest that there is no shortage of potential generators of significant and tsunamigenic submarine landslides within a vicinity that can affect the Diablo Canyon site.

For these reasons, this study focuses on locally generated tsunami scenarios due to potential submarine landslides that may occur offshore along the continental slope and shelf between, at the northern end, Pt. Lobos (near Carmel) and, at the southern end, Point Conception (west of the Goleta / Santa Barbara area). This region is shown in Figure 1. Although there are other potential (distant and local) tsunami generators that should also be considered in a state-of-the-art tsunami hazard analysis of the Diablo Canyon site, the issue of locally generated landslide tsunamis is believed to be of greatest significance from the standpoint of potential non-conservatism in the existing tsunami analyses and design basis.

3. Overview of this Study

This study considers tsunami events and characteristics that are based on general time frames, or return periods, that are relevant to the design basis and beyond-design-basis performance/margin of nuclear power plants. For design bases, a typical time frame of at least 5,000 to 10,000 years is considered applicable (e.g., such time frames are consistent with nuclear power plant design for seismic ground motions), whereas for performance/margin, a time frame of at least 100,000 years is considered applicable (i.e., nuclear power plant safety goals imply no shorter than a 10,000 year repeat time for core damage from all accident causes; the core damage repeat time due to any individual initiator, such as tsunamis, should be much longer[3]). A truly probable

[3] In the Individual Plant Examination of External Events (IPEEE) program, initiators known as HFO (high winds, floods, and other) events could be screened out by showing that the mean risk of core damage due to the initiator would be less than 10^{-6} per reactor-year, which means a core-damage repeat time of not shorter than 1,000,000 years for each initiator. This clearly shows that, in the regulatory context of safety management, there is validity to considering individual initiating events with repeat times up to 1,000,000 years.

Aside from safety against core damage, there are also goals for safety against large radiological release (e.g., from containment breach or bypass) and offsite consequences. For instance, a one-in-ten chance of large radiological release given core damage is typically applied, and thus, the subset of scenarios (for a given initiating event maximum event (i.e., one having repeat time significantly in excess of 1,000,000 years, or one with virtually no chance of being exceeded – as typically serves as the basis for deterministic design) is likely to have characteristics more severe than those developed here. On the other hand, the events considered here should be based on time frames significantly longer than those covered by the historical record of regional events (e.g., the 1964 distantly generated tsunami at Crescent City, CA of 17 to 20 ft; the 1812 locally generated tsunami at Goleta, CA estimated at 33 ft; and various other California tsunamis in the historical record/database), and they may also be significantly greater than events considered in other studies (e.g., tsunami inundation mapping, evaluation planning, etc.) that did not have the purpose of being used in the safety analysis of a critical facility.

Although this study selects scenarios keeping in mind their potential time frames (which can through suitable analysis be linked to return periods obtainable from probabilistic methods), this study is still deterministic in that it looks at a fixed set of scenarios and develops tsunami characteristics based on deterministic analysis for those scenarios. A full probabilistic tsunami hazard analysis would develop a more comprehensive set of tsunami scenarios (from all meaningful tsunamigenic sources/causes), estimate their likelihoods, produce a probabilistic synthesis of results, and evaluate uncertainties in the tsunami hazard estimates based on interpretation of various experts (e.g., similar to what was done in the NRC/LLNL probabilistic seismic hazard analysis program).

In addition to peak positive and negative wave amplitudes, modern tsunami design bases should also develop water particle velocities, as these are important factors in design and failure analyses. In engineering analyses, time histories of wave amplitudes and (x, y) water particle velocities are typically needed or, at least, very useful. For the scenarios considered in this study, such results have been generated.

This study is based on numerical simulation of the landslide tsunami scenarios. Such simulation includes the following three elements: (1) generation of the landslide source and initial water disturbance; (2) propagation of the wave from the source through open water; and (3) interaction of the wave with the local shore (including amplifications due to shoaling) for evaluating run-up

category, such as tsunamis) found to be capable of leading to large radiological releases should have, on average, a repeat time roughly ten times as long as that for the set of scenarios capable of producing core damage.

and draw-down.[4] Among tsunami scientists, each of these factors generally pertains to a distinct expertise, and there exist a variety of data and methods to address each aspect. To keep the simulations for this study manageable, relatively simple models that are yet representative of tools typically employed (and that have previously been employed) in tsunami hazard studies are used. To provide a check on results and better understand variations in results that may derive from numerical modeling approaches, two independent programs were used to evaluate the combined elements of wave propagation and wave-shore interaction.

Information on submarine geology, geomorphology, geotechnical properties, and other factors affecting slide potential along the north-central to south-central offshore region of California were not readily available. (Indeed, collection of such data in addition to very high resolution [VHR] bathymetry appears to be a significant need.) Therefore, for this study, slide characteristics were based on simple geometric parameters such as slide area and volume, and simplified physical parameters such as average slide velocity (magnitude and vector orientation), as estimated in consideration of scientific studies summarizing characteristics of past submarine landslides. Although the landslide scenarios here were thus not generated based on geotechnical properties and a detailed physical model incorporating such properties, the slide characteristics are site specific in the sense that their locations, shapes, and slide velocities were chosen based on detailed visual analysis of the bathymetry, so as to be reasonably consistent with expected and potential physical behavior.

Since detailed elevation data for developed features/facilities was not available in the near vicinity onshore and offshore of the Diablo Canyon site, a detailed local analysis could not be performed of tsunami wave interaction with the offshore breakwaters and onshore structures, grades, etc. Rather wave amplitudes were obtained in the very near offshore (at 2.7 m to 3.4m water depth), and for the purposes of this study the peak wave run-up elevation onshore can be estimated at about 25 to 50 percent greater than the peak positive wave amplitude at this near-offshore location[5].

The wave amplitudes evaluated in this study are with respect to mean sea level (MSL). This study does not include other wave effects such as tide variations, storm surge, wind-induced waves, etc. The predominant dynamic period of tsunami waves produced from local submarine

[4] These factors are directly analogous, respectively, to the following factors in seismology: (1) seismic source and ground rupture modeling: (2) seismic wave propagation modeling; and (3) site response modeling.

landslides is typically much shorter than for tsunamis produced from distant earthquakes. As a first approximation, the interaction of wave effects can be estimated by simple superposition (i.e., summation of the tsunami wave with tidal, storm surge, and wind-induced effects), however, a detailed hazard assessment would need to give more detailed treatment to wave interactions.

Owing in large part to the limited data and approximations as noted in this section (and elsewhere in this summary report), this study is considered to be a preliminary assessment of the tsunami hazard at the Diablo Canyon site for locally generated tsunamis. The analysis is believed to be suitable to draw the conclusions and recommendations documented subsequently.

A brief summary of each of the major aspects of the present study is provided below, and includes the following topics:

- Collection and processing of elevation data
- Recent information pertaining to landslide tsunamis
- Software acquisition, preparation, and development
- Three-dimensional visual analysis and submarine landslide scenario identification
- Description and analysis of tsunami scenarios
- Summary of numerical simulation results
- Potential implications of results
- Conclusions and recommendations

4. Collection and Processing of Elevation Data

This study started with the collection of elevation data, including both offshore bathymetry and land topography. Recent studies of known submarine landslides (e.g., offshore southern California) have been based on VHR bathymetry data, as acquired for example from multi-beam echosounder systems (MEBS). Such data for the area considered in this study were not available, and most likely have not yet been obtained for much of the region of interest for this study. Although the elevation data used in this study are in the public domain, considerable effort was nonetheless expended in searching, acquiring, and processing the data for this project.

---

[5] However, the factor may potentially be higher (e.g., information presented by Geist [1999] and Watts [2003]

Readily available, public-domain worldwide digital elevation data include 5-minute and 2-minute data sets for bathymetry, and 30-second data sets for topography. Although frequently used for transoceanic and regional tsunami analyses, such data are of rather low resolution having limited applicability for local tsunami analyses. Higher resolution data can be obtained from navigation and oceanic survey charts, but requires the effort of extensive digitizing.

The bathymetry data ultimately obtained for this study was acquired from the California Department of Fish and Game (CDFG). The CDFG has expended considerable effort in synthesizing a large set of data from several sources, including digitized charts, and have converted the data into their geographic information system (GIS) in the ESRI ArcView format. In support of the scientific nature of this study, they furnished the data for this project on a set of 10 CD-ROMs at no charge. The data were provided in sets at various horizontal resolutions ranging from 200 m to 5 m, however, those are the digitized resolutions and the actual resolution of the original data varies. In addition, at the time the CDFG provided the bathymetry data, they were in the process of converting the elevations to a common datum, and so the data they provided has some mismatches from joining results from different surveys/charts. (One can see such mismatches in maps and images of the data, however, their effect on the tsunami results developed in this study is considered to be negligible. In fact, the accuracy of the CDFG data appears to be very much better than that from alternative public-domain sources.) CDFG provided the bathymetry data in the form of ESRI grids, whereas an ASCII format is needed for purposes of input to programs that perform numerical tsunami simulation.

The GIS group at the Center for Nuclear Waste Regulatory Analyses (CNWRA) imported the CDFG data volumes (as ESRI grids) into the ArcInfo software, and combined bathymetry data of approximately 25 m horizontal resolution with California land topography data of about 20 m resolution (obtained from http://www.gis.ca.gov/). CNWRA converted the elevation data layers into ASCII format, producing four files totaling nearly 2 GB of elevation data.

The ASCII data files produced by CNWRA were used as the raw data for developing imaging and computational grids covering the region of interest for this study. A Fortran program was written to extract the raw data and convert it to uniform latitude-longitude grids (for imaging) or uniform x-y grids (for computation) of selected resolution (having spacing equal or exceeding 25 m). Resolution of imaging and computational grids varied from 100 m to 500 m, depending upon the size of the landslide feature(s) under consideration. Several grids, covering different

suggest that the ratio of peak run-up to peak amplitude at shoreline may exceed a factor of 2).

sub-areas of interest, were developed. This development of gridded sub-areas at different resolutions was necessary to obtain manageable visual and computational grids.

The extracted data were then used as input to the Generic Mapping Tool (GMT, Wessel and Smith, 2003) set of utilities to obtain 3D images for visualization, 2D contour plots, and x,y,z ASCII data formatted for input to the numerical tsunami analysis programs.

5. Some Recent Information Pertaining to Landslide Tsunamis

In recent years, there has been accelerated growth in the body of peer-reviewed scientific and engineering literature concerning submarine landslides and landslide tsunamis. Greater recent attention to the threat of landslide tsunamis has also been seen in the media and non-peer-reviewed sources, with correspondingly greater public awareness of this hazard. Apparently, the 1998 Papua New Guinea tsunami has been a particularly pivotal event in such developments. The resulting growth in scientific understanding and public awareness of the landslide tsunami threat will undoubtedly increase expectations concerning the evaluation of such events in the safety analysis of critical facilities.

A landslide tsunami workshop, sponsored by the National Science Foundation (NSF), was recently held at the University of Hawaii at Manoa on 30–31 May 2003, and was attended by a group of over 40 experts in this field. This workshop provided an overview of past landslide tsunamis, and focused on topics related to the latest methods for numerical modeling of these events. The author of the present study participated in that workshop, and to the extent possible has incorporated that most-recent information in the selection and modeling of landslide tsunami scenarios for this study. It is important to note, however, that as for most areas of science, there are considerable differences in expert interpretations leading to variations/uncertainties regarding landslide tsunami hazard.

At this point in time, the landslide tsunami threat for offshore central California has not yet been well studied, nor does it yet appear to be well understood. As noted previously, much attention has been given recently to the landslide tsunami potential in the more populated region of southern California. Investigations have been performed in relation to the 1812 submarine landslide offshore of Goleta, CA. According to some, in the near vicinity of that historical slide, there exists the potential in the foreseeable future for a similar or larger event occurring and producing perhaps peak wave amplitudes of about 50 ft [+15.2 m] onshore (Synolakis, 2000).

Submarine landslides of moderate size have also been mapped using recently acquired VHR bathymetry, off the peninsula near Palos Verdes, CA. Two particularly "sharp, fresh" landslide deposits have been identified, with one being dated at 7,500 years, and the other believed to be relatively recent (Lee et al, 2003). Hence a recurrence time of roughly a few thousand years can be estimated for significant landslide events offshore Palos Verdes. Due to the considerable distance of debris travel, at least one of those scenarios was estimated to have an initial velocity exceeding 40 m/s [89 mph], with offshore amplitude of at least 8 m at the source (Locat et al., 2003); potential future events in the area were estimated to be capable of producing onshore wave heights of at least 100 ft [+30.5 m] (Locat, as quoted by the press).

Significant attention has also been given to the tsunami threat for coastal southern Oregon. Goldfinger et al. (2000) document super-scale failures (submarine landslides) of the southern Oregon Cascadia margin, and infer three such super-scale events from available evidence, with dates of about 110 kya, 450 kya, and 1210 kya (approximate repeat time of 400,000 years for such super-scale failures). Taken together, the three slide scarps have an estimated area of 8,000 km^2 and a volume of 12,000 to 16,000 km^3 (implying an average slide depth of about 1500 to 2000 m). They traveled about 25 to 70 km onto the abyssal plain, and were most likely triggered by large subduction earthquakes. A separate study by Hemphill-Haley and Lewis (2003) found evidence for 13 separate occurrences of significant coastal tsunami inundation in south-central Oregon (at Bradley Lake) over the past 7,200 years (return period of about 550 years). Given the super-scale failures experienced in the geologic past in this area, and ongoing sedimentation, it is most likely that at least some of these events were caused or accompanied by a significant degree of submarine landsliding.

Similar investigation of landslide tsunamis can be cited for areas such as Washington, Alaska and Hawaii, in addition to locations outside the U.S. Given the lack of detailed investigation for offshore central California, such investigations have applicability in this study at least in terms of the characteristics of scenarios that have occurred elsewhere and that cannot be immediately ruled out without further investigation. Some key characteristics and points of information gleaned, for use in this study, from the scientific literature and scientific discussions include the following:

- Submarine landslides and landslide tsunamis occur worldwide, and the potential for large events apparently increases with the degree of sediment accumulation and local gradient.

Various causes can serve as landslide triggers, but earthquakes appear to be one of the most significant triggers.

- Wave amplitude from landslide tsunamis generally increases as the landslide velocity approaches the depth-depended natural wave celerity (reasonably approximated as $c=\sqrt{(gd)}$ where g is acceleration due to gravity and d is the water depth).

- Although of considerable debate among scientists, landslide velocities ranging from 8 m/s (for a short slide) to 200 m/s (for a very long slide) are believed to be possible based on observation and theory (Watts, 2003). Other experts interpret that the empirical physical evidence supports maximum slide velocities of about 60 m/s (Keating, 2003) or about 100 m/s (Day, 2003) as being more representative.[6]

- Large continental slope/shelf failures of up to a few thousand square kilometers in area and several thousand cubic meters in volume have occurred, and have probably been triggered by large earthquakes.

- Moderately large submarine slides have areas up to hundreds of square kilometers and volumes up to perhaps a few hundred cubic kilometers.

- Information from Watts (2002) suggests representative slide thickness is about 10 to 15 percent of the slide length (in direction of travel). Watts (2002) also provides probabilistic estimates of offshore/source tsunami amplitude for southern California, based on empirical data and on simulations, and indicates that onshore run-up is likely to be about twice the offshore/source amplitude (Watts, 2003). For numerical modeling of submarine landslide tsunamis, Watts (2002, 2003) indicates that solid block modeling of the sliding wedge produces reasonably accurate results; the more realistic case of mass dispersion generally alters the wave amplitudes by only about 10 percent.

The foregoing are very general points, and serve as reasonable rules of thumb for characterizing landslide tsunami scenarios in a preliminary analysis such as the present study. A more detailed hazard assessment would investigate these points more fully, perhaps by means of sensitivity analysis.

6. Software Acquisition, Preparation, and Development

The public-domain programs SWAN (Mader, 1988) and TUNAMI-N2 (Imamura et al., 1991, as subsequently revised by Watts) were obtained for use in this study to solve the equations for tsunami wave propagation and near-shore wave interaction. These programs use the finite-difference method to solve the two-dimensional nonlinear shallow-water equations of fluid dynamics. They include nonlinear terms and features needed to model wave-shore interaction (such as near-shore shoaling). Both programs have been frequently cited in the published literature with respect to tsunami analysis including landslide tsunamis. The SWAN program incorporates onshore flooding using an algorithm that essentially approximates a "porous boundary" that allows wave effects (amplitude and velocities) to penetrate finite-difference grid points corresponding to land.

More sophisticated models include those that solve the full (3D or 2D) Navier-Stokes equations or that include higher order (e.g., dispersion) terms of the Bousinessq equations, and/or that include an explicit porous boundary for modeling wave run-up. Although not the case with TUNAMI-N2, the SWAN code does solve a form of the 2D Navier-Stokes equations that incorporates the advection, Coriolis, and friction terms.

A program LS-SOURC that generates the three-dimensional landslide source (Sewell, 2003) was used for modeling the sea-bottom movements leading to the initial wave disturbance. This program is based on geometric algorithms that model any specified shape of the failure (mass-cutting) plane and propagate the (bathymetry dependent) failure mass along a specified down-slope trajectory at specified path-dependent velocity. LS-SOURC was embedded within the SWAN code, which can accommodate bottom motions; the modified version of the SWAN code is here called LS-TSUN. The TUNAMI-N2 code takes an initial wave-height disturbance as input, but does not readily accommodate a bottom motion. Hence, the wave disturbance computed from LS-TSUN at the time that the landslide movement is complete was used as input to TUNAMI-N2. LS-TSUN was modified to output grid wave heights and (x, y) water particle

[6] The issue of peak submarine slide velocities among tsunami scientists is reasonably analogous to the issue in earthquake science of defining limiting parameters that influence peak ground motions.

velocities. TUNAMI-N2 accepts only grid wave heights, but was modified in this study to also accept the grid of (x, y) water particle velocities, in order to fully input the wave disturbance.

Both LS-TSUN and TUNAMI-N2 were subject to test analyses to insure that the compiled and linked code (executable) performed as expected on the Windows XP platform.

Output from these programs include both time-dependent results of the entire solution grid (useful for developing wave animations), as well as wave amplitude and velocity time histories and/or peak values at specified grid-point locations. The gridded output files were processed using the GMT utilities to obtain 3D images and 2D contours of the wave heights (for wave animation) and bottom motions (for landslide animation).

7. Three-Dimensional Visual Analysis and Submarine Landslide Scenario Identification

In order to identify locations and configurations of potential submarine landslides within the study area, a variety of visualization products were prepared, including color images and contour plots of the bathymetry. For each data grid (covering a given sub-area of the overall region of interest), several 3D color images were generated and examined, corresponding to various viewpoint orientations/perspectives and illuminations. Generating and examining the visual images proved to be a time consuming task, but a very useful one for identifying likely areas of erosion, sediment accumulation, and past sliding/slumping, and for examining areas having steep gradient. Figure 2 shows example 3D bathymetry images for two past slides (Goleta slide and a slide off of Point Sur), and Figures 3 and 4 show some sample 3D images of bathymetry covering the study region (these later figures are not representative of the finer detail at which the bathymetry data were examined for identifying submarine landslide scenarios).

For specific zones where a more quantitative examination of the bathymetry was needed – such as for defining the cutting-planes that would determine the configuration of sliding mass for a given landslide scenario – contour plots having small contour intervals were prepared. Based on judgment, boundaries of the sliding mass were drawn on these contour plots, and the boundaries were digitized to obtain inputs into the landslide generator (LS-SOURC)[7].

[7] A more sophisticated analysis would involve searching multiple failure surfaces, computing safety factors against sliding (both in the case of static and dynamic loading), and selecting the most likely failure surface based on lowest factor of safety. Such effort would require detailed geotechnical/geophysical data to implement, which although

From this evaluation, 13 landslide scenarios were developed. These cases were not selected to be exhaustive or to necessarily reflect the most likely landslide locations. Indeed, an essentially infinite array of possible slide configurations could be conceived and the most likely landslide locations may not necessarily be the most tsunamigenic or representative of tsunami hazard for the time frames of interest. The 13 cases were, rather, chosen as a "sample" of events that (a) are placed at credible locations considering the bathymetry; (b) have credible characteristics (area, volume, depth, velocity, etc.) that are consistent with both the bathymetry data and characteristics of significant submarine events identified/studied elsewhere; (c) have, in consideration of the limited available data, credible characteristics considering the time frames of interest for design and performance evaluation of nuclear power plants; and (d) may be sufficiently tsunamigenic to present a potential challenge to the Diablo Canyon site. In other words, these scenarios are a sample of events that could suggest, without the benefit of evidence or analysis to the contrary, that the tsunami threat to the Diablo Canyon site, relative to the design bases and possibly the beyond-design-basis performance (i.e., risk), may be higher that previously thought, and not insignificant. It is likely that, given further investigation (e.g., development and analysis of VHR bathymetry, submarine geologic/geomorphic examination, and/or submarine geotechnical investigation) some of the chosen scenarios will be confirmed as being applicable and others may be ruled out. It is not the purpose of this study to develop final conclusions regarding the local landslide tsunami hazard, and final conclusions concerning such hazard should not be drawn from the 13 scenarios. As stated previously, the 13 scenarios are intended to serve as basis for demonstrating whether or not a detailed tsunami evaluation appears to be warranted.

8. Description and Analysis of Scenarios

Figures 5 and 6 show the locations of the sample of 13 submarine landslide scenarios developed in this study, and Table 1 summarizes key characteristics for these landslides.

The characteristics of slides in Table 1 are well bracketed by the range of values recently presented and discussed by tsunami scientists. They can (in terms relative to scenarios of interest) be generally described as moderately small to large events, and based on the limited

outside the scope of the present preliminary study would be important in a detailed landslide tsunami hazard investigation. Such effort would clearly refine the assessment. However, the overall size, shape, and velocity of the information available, they are proposed here as being representative of time frames – depending upon the specific event – ranging from hundreds of years to perhaps many hundreds of thousands of years (say, 250 years to 500,000 years). Furthermore, triggers for such events are most likely to be large and/or close earthquakes that may induce high dynamic loads (including possible near-source effects, topographic effects, etc.), fault offsets, increased pore pressures in sediments, significant release of trapped gases, or a combination of these effects in the near vicinity of the slide. Indeed these conditions are likely to be realistic for large earthquakes, and the scenario slide locations are in near vicinity to several known active and capable faults.

The geometric properties of the slide scenarios presented in Table 1 are most closely related to the bathymetry. The travel distances and velocities noted in Table 1 are consistent with values noted in scientific investigation and discussion. However, they were in some cases selected, or constrained, to keep computations manageable or to evaluate sensitivity. For instance, the most consistent interpretation for Scenarios No. 7 to 9 would be that the slides continue for perhaps 50 to 60 km onto the abyssal plain. This interpretation would likely produce somewhat greater tsunami effects for Scenario No. 7 and perhaps significantly greater effects for Scenarios 8 and 9. However, the computational grid would have to cover a much greater area to capture this additional motion, and either the computation time would become very large (for the same grid resolution) or accuracy would be sacrificed by going to a lower resolution grid. For Scenario 7, most of the effect of the landslide is likely captured. Scenarios 8 and 9 can be interpreted as more limited slides (with more limited effects, and correspondingly shorter repeat times). A related situation worth noting in the numerical analysis of these scenarios is that some of the scenario slides extend close to the edge of the computational grids before the full momentum transfer of the wave in the direction of the site may have been realized. Although numerical re-evaluation and/or sensitivity analysis for some of the scenarios would be desirable in preparing final analyses, as will be seen later, the conclusions produced from this study will not be affected.

Additionally, as discussed in the scenario descriptions to follow, the thickness of slides in this study tend to be somewhat lower than what has been reported as characteristic for past slides. In other words, it would be probably somewhat more realistic to generate slides with greater thickness. Increasing slide thickness for the scenarios would increase slide mass/momentum and produce more significant wave effects. Again, although numerical re-evaluation and/or

sliding mass capture the dominant tsunamigenic character, and the sliding surfaces developed herein are believed to be reasonably and practically suitable for that purpose.

sensitivity analysis pertaining to slide thickness may be desirable (any final tsunami hazard assessment for the Diablo Canyon site should include such refinements), the conclusions produced from this study remain unaffected.

Given the limited information available, the selected scenarios, scenario characteristics, and their analysis are otherwise considered to be reasonably realistic for the proposed time frames. Selection of more severe or less severe slide configurations would clearly be possible within the limits of current scientific uncertainty in tsunami landslide characteristics.

Following is a brief summary of important information specific to each tsunami scenario and its analysis:

Scenario No. 1

This moderate-size slide is in very near proximity to the Santa Lucia Bank Fault. Local gradients are moderate, with average slope of about three percent and maximum slope of about six percent. The slope is at the western end (high) of the Santa Maria Basin, and is one of few local cases where sliding would be oriented toward the shoreline at the Diablo Canyon site. Direction of slide propagation is toward the northeast, following a local gradient into the Santa Maria Basin. (Scenario 1 is the only case in this study where the slide propagates directly toward the coastline at Diablo Canyon. For Scenarios 2 to 12, all slides propagate [and have momentum directed] toward the open sea, away from the Diablo Canyon site. For Scenario 13, the slide propagates toward the south-southwest.) The slide was taken to be comparatively thin (44 m average height; 79 m peak height, which is less than one percent of its width in the direction of slide propagation), with corresponding limits on momentum, reflecting the judgment of lower sediment accumulation over this area.

For tsunami wave analysis, Scenario No. 1 was analyzed using a computational grid spanning longitudes from -121.50 to –120.50 and latitudes from 34.75 to 35.50, and having a uniform grid-point spacing of 200 meters.

Scenario No. 2

This moderately small slide is in very near proximity to the Hosgri Fault, and extends from the near (<5 km) offshore area of Diablo Canyon to the southern mouth of Estero Bay. The slope is at the eastern end of the Santa Maria Basin. This is the slide scenario that (in this study) is closest to the Diablo Canyon site. Local gradients are moderately low, to moderate, with average slope of about three percent and maximum slope of somewhat over four percent. The head of the slide is positioned just above an area where a predominant break in the slope (possibly along the local alignment of the Hosgri Fault) can be observed from 3D images. Direction of slide propagation is largely toward the west, following a local gradient into the Santa Maria Basin. The slide was taken to be comparatively thin (27 m average height; 63 m peak height, which is less than one percent of its width in the direction of slide propagation), in consideration of the moderate gradient and vertical elevation difference of the break in the slope.

For tsunami wave analysis, Scenario No. 2 was analyzed using a computational grid spanning longitudes from -121.25 to –120.60 and latitudes from 35.00 to 35.50, and having a uniform grid-point spacing of 100 meters.

Scenario No. 3

This moderately large slide lies within the Santa Lucia Bank Fault zone, south of the Santa Lucia High, at the upper reaches of the continental slope. Local gradients are moderately high, to high, with average slope of about six percent and maximum slope of somewhat over 15 percent. The head of the slide is positioned just above an area where a predominant break in the slope can be observed from 3D images. Images and transition in contours below the area of the major gradient change suggest sediment accumulation and potential slide/slumping debris. At their lower reaches lies a U-shaped basin; this basin resembles a bathymetric feature ("amphitheatre" shaped depression) that evidence suggests produced the 1998 Papua New Guinea tsunami. Direction of slide propagation is toward the southwest, following a local gradient into the U-shaped basin. The slide is moderately shallow (221 m average height; 564 m peak height, which is 2.6 percent of its width in the direction of slide propagation), reflecting the local gradient, vertical elevation difference at the major change in gradient, and possible sediment/debris accumulation.

For tsunami wave analysis, Scenario No. 3 was analyzed using a computational grid spanning longitudes from -122.00 to –120.50 and latitudes from 34.00 to 35.50, and having a uniform grid-point spacing of 400 meters.

Scenario No. 4

This moderately large slide lies within the southern reaches of the Santa Lucia Bank Fault zone, at the upper extent of the continental slope. The slope delineates the eastern border of a submarine valley/canyon. Local gradients are moderately high, to high, with average slope of about six percent and maximum slope of somewhat over 15 percent. The head of the slide is positioned just above a locally steep area. Images and transition in contours below this area strongly suggest slide/slump debris (extending to near the lower extent of the continental slope). Direction of slide propagation is toward the southwest, generally following the local gradient but constrained by the relatively steep borders of the valley/canyon below. The slide has thickness somewhat less than representative slides (548 m average height; 820 m peak height, which is about 5.5 percent of its length in the direction of slide propagation), reflecting the local gradient, vertical elevation difference at the major change in gradient, and the size of possible slide/slump debris below.

For tsunami wave analysis, Scenario No. 4 was analyzed using the same computational grid parameters as noted for Scenario No. 3.

Scenario No. 5

This moderately large slide lies on the west side of the Santa Lucia Bank Fault zone, below the area of the slide for Scenario No. 3, extending to the lower reaches of the continental slope. Local gradients are high, with average slope of about ten percent and maximum slope over 20 percent. The slide is at the northwest end of the U-shaped basin discussed previously for Scenario No. 3. This region of the basin bulges somewhat down slope (toward the southeast) in comparison to the relatively linear slopes to the north and south, and (in images and contours) has the appearance of being potentially less stable than the surrounding walls of the U-shaped basin. It also represents a case of potential failure of continental margin on a relatively small scale (e.g., as compared to Scenarios No. 7 and 9). Direction of slide propagation is toward the southwest, following a local gradient toward the abyssal plain. The slide is moderately shallow (279 m average height; 625 m peak height, which is about four percent of its length in the direction of slide propagation), as compared to characteristic slide parameters (i.e., generic ratio of peak height to length of about 10 to 15 percent).

For tsunami wave analysis, Scenario No. 5 was analyzed using the same computational grid parameters as noted for Scenario No. 3.

Scenario No. 6

This moderately large slide lays at the southern part of the Santa Maria Basin, offshore of Pt. Arguello, along a comparatively steep portion of the continental shelf that makes transition toward the east into the (comparatively steep) slope that defines the northern edge of the Santa Barbara Channel. There are a number of faults within this area, and the M_S 7.0 tsunamigenic earthquake of 4 November 1927 occurred (epicentral location) within the boundary of this slide scenario. Erosion features are apparent within the upper extent of this slide, and a wedge of significant sediment accumulation, leading down-slope toward the submarine valley/canyon, as noted in the description of Scenario No. 4, is apparent. Local gradients are moderately high, to high, with average slope of about four percent and maximum slope of about 10 percent. The head of the slide is positioned just above a locally steep area encompassing the erosion features. Direction of slide propagation is toward the southwest, following the local gradient into the valley/canyon below. The slide is relatively thin (107 m average height; 233 m peak height, which is less than one percent of its length in the direction of slide propagation); the gradient and apparent sediment accumulation could likely justify a significantly deeper slide.

For tsunami wave analysis, Scenario No. 6 was analyzed using the same computational grid parameters as noted for Scenario No. 3.

Scenario No. 7

This very large slide occurs along the Santa Lucia Escarpment that defines a significant portion of the continental slope. The slide is significantly smaller than – but yet for this study comes closest to approaching – the size of the super-scale continental margin failures noted in southern Oregon. Such a slide would likely require an unusually powerful local earthquake, and correspondingly, the expected time frame for such an event is long. Scenarios No. 8 and 9 involve continental margin failures of, respectively, somewhat smaller scale and lower extent of mobilization than Scenario No. 7, and would thus be associated with shorter time frames. Local gradients in the area encompassed by the slide of Scenario No.7 are very high, with average slope of about 15 percent and maximum slope exceeding 30 percent. Direction of slide propagation is toward the southwest, following the local gradient toward the abyssal plain. The slide has nearly representative thickness (696 m average height; 1450 m peak height, which is about eight percent of its length in the direction of slide propagation), just somewhat smaller than characteristic slide parameters (i.e., generic ratio of peak height to length of about 10 to 15 percent).

For tsunami wave analysis, Scenario No. 7 was analyzed using a computational grid spanning longitudes from -122.50 to –120.50 and latitudes from 34.00 to 35.75, and having a uniform grid-point spacing of 400 meters.

Scenario No. 8

This large slide occurs just north of the slide for Scenario No. 7, along the continental slope, and on the western side of the Santa Lucia Bank Fault Zone. The slide is significantly smaller than Scenario No. 7, and has more limited movement. However, such scale of sliding would still likely require a powerful local earthquake. There is evidence in the imaging and contours for significant ongoing sediment accumulation (coming from the Santa Lucia High/Bank above). Local gradients are high, with average slope of about 5 percent and maximum slope of about 15 percent. Direction of slide propagation is toward the west-northwest, following the local gradient toward the abyssal plain. The slide is non-representatively thin (287 m average height; 838 m peak height, which is about two percent of its length in the direction of slide propagation).

For tsunami wave analysis, Scenario No. 8 was analyzed using the same computational grid parameters as noted for Scenario No. 7.

Scenario No. 9

This large slide occurs just north of the slide for Scenario No. 8, along the continental slope, and on the western side of the northern extent of the Santa Lucia Bank Fault Zone. The slide is similar in size to Scenario No. 7, but with much more limited movement. Imaging and contours reveal that sediments from the Santa Maria Basin are being fed into this area, with the source of these deriving particularly from the vicinity of slides for Scenarios 10 to 12. Local gradients are high, with average slope of about 6 percent and maximum slope of about 25 percent. Direction of slide propagation is toward the southwest, following the local gradient toward the abyssal plain. The slide is relatively thin (614 m average height; 1280 m peak height, which is about three percent of its length in the direction of slide propagation).

For tsunami wave analysis, Scenario No. 9 was analyzed using the same computational grid parameters as noted for Scenario No. 7.

Scenario No. 10

This moderately small slide lies offshore of Cambia, CA in near proximity to the San Simeon Fault Zone, and relatively close to the Diablo Canyon site. It is the smallest slide considered in this study. It is somewhat similar in size (yet still relatively smaller) than slides observed on the slopes of the Santa Barbara Channel and offshore of the Palos Verdes Peninsula having historical or geologically recent time frames (about 200 to 3000 years). Such a slide at the scenario location would most likely be triggered by an earthquake on a nearby fault, and so would be expected to have a time frame governed by the local seismicity. Local gradients are low, to moderate, with average slope of just over two percent and maximum slope of somewhat over four percent. The head of the slide is positioned just above an area where a predominant break in the slope (possibly along the local alignment of the San Simeon Fault) can be observed from 3D images. Direction of slide propagation is toward the southwest, following a local gradient into the Santa Maria Basin. The slide was taken to be comparatively thin (22 m average height; 105 m peak height, which is less than one percent of its width in the direction of slide propagation), reflecting the moderate gradient and vertical elevation difference of the break in the slope.

For tsunami wave analysis, Scenario No. 10 was analyzed using a computational grid spanning longitudes from -122.00 to –120.60 and latitudes from 35.00 to 36.00, and having a uniform grid-point spacing of 200 meters.

Scenario No. 11

This moderately large slide lies offshore of Pt. Piedras Blancas in near proximity to the San Simeon Fault Zone. This slide has erosion features / gullies at its northern and southern ends, and the images and contours suggest bulging at its lower (southwest) end and subtle evidence of extension at its upper (shoreward) end that may indicate a very marginal factor of safety against sliding. Local gradients are moderate, to high, with average slope of just over three percent and maximum slope of somewhat over 10 percent. The head of the slide is positioned with the alignment of extension features, just somewhat above the area where the predominant break in the slope (possibly along the local alignment of the San Simeon Fault) is seen. Direction of slide propagation is toward the southwest, following a local gradient into the Santa Maria Basin. The slide was taken to be comparatively thin (111 m average height; 316 m peak height, which is about 1.5 percent of its width in the direction of slide propagation), but not inconsistent with the vertical elevation difference at the break in the slope.

For tsunami wave analysis, Scenario No. 11 was analyzed using the same computational grid parameters as noted for Scenario No. 10.

Scenario No. 12

This moderate-size slide lies offshore of Ragged Pt. in near proximity to the San Simeon Fault Zone. This slide occupies the northeast sub-region of the Scenario No. 11 slide, in consideration of the potential for sliding in this vicinity to have varying size, between that for Scenarios No. 10 and 11. This slide encompasses the relatively more severe gradient and erosion features within the Scenario No. 11 slide. Local gradients are moderate, to high, with average slope of almost four percent and maximum slope of somewhat over 10 percent. Direction of slide propagation is toward the southwest, following a local gradient into the Santa Maria Basin. The slide was taken to be comparatively thin (91 m average height; 338 m peak height, which is less than two percent of its width in the direction of slide propagation), but not inconsistent with the vertical elevation difference at the break in the slope.

For tsunami wave analysis, Scenario No. 12 was analyzed using the same computational grid parameters as noted for Scenario No. 10.

Scenario No. 13

This large slide lies offshore of Pt. Sur in near proximity to the Sur Fault segment that lies between the San Simeon Fault Zone (to the south) and the San Gregorio Fault Zone (to the north). The offshore canyon is just to the south of, and has features (in terms of size and gradient) similar to, Monterey Canyon, a known active generator of significant submarine landsliding. Landslides generated at this location can be expected to have somewhat greater tsunamigenic effect at the Diablo Canyon site, as compared to those (given similar size and configuration) generated within Monterey Canyon. A significant existing region of sliding/slumping within, and immediately to the north of, the Scenario No. 13 area can be easily seen in contours and 3D images of the bathymetry. Local gradients in this area are high, to very high, with average slope of about five percent and maximum slope exceeding 30 percent. The head of the slide is positioned just above an area where a predominant break in the slope can be seen, and near the head scarp of the existing slide just mentioned. Direction of slide propagation is toward the south-southwest, following a local gradient into an adjacent region of the continental slope. The slide was taken to be thin (485 m average height; 876 m peak height, which is about 2.4 percent of its length in the direction of slide propagation).

For tsunami wave analysis, Scenario No. 13 was analyzed using a computational grid spanning longitudes from -123.00 to –120.60 and latitudes from 35.00 to 37.00, and having a uniform grid-point spacing of 500 meters.

9. Summary of Numerical Simulation Results

Table 2 provides a summary of the peak positive and negative wave amplitudes, with respect to MSL[8], as calculated for two sites in the near-shore vicinity of Diablo Canyon. Site No. 1 is about 1 km offshore from Site No. 2 (0.9 to 1.2 km, depending upon the computational grid size), following a direction perpendicular to the local shoreline. Water depth at this location is about 35 meters [114 ft] (exact depth varies slightly depending upon the computational grid size). Site No. 2 is very near the shoreline at a water depth of about 3 meters [9.8 ft] (depending upon the computational grid size, the depth varied from 2.7 to 3.4 meters [8.9 to 11 ft]); for each numerical simulation, this location was defined by the offshore grid-point closest to the DCPP site.

Values provided in Table 2 include results obtained from the LS-TSUN and TUNAMI-N2 programs. A value of "BOT" for peak negative wave height indicates that the wave bottomed out at the indicated location, and correspondingly, the wave receded below that level. Due to the limited grid coverage, and the fact that input to TUNAMI-N2 is developed as the wave configuration determined from LS-TSUN at the time the landslide movement is complete, TUNAMI-N2 wave amplitudes could not be obtained for Scenario No. 7. Hence, no values are provided for this case in Table 2.

[8] Add 2.6 ft [0.79 m] to the peak amplitudes provided in Table 2 to obtain peak amplitudes with respect to MLLW.

Figures 7 to 19 provide time histories of wave amplitude for all 13 tsunami scenarios at Sites No. 1 and 2. Time history results of wave amplitude are provided for both the LS-TSUN and TUNAMI-N2 programs.

In addition to these results, for each scenario "snapshots" of the 3D propagating landslide configuration and the propagating tsunami wave were obtained from the analyses at regular, specified time intervals. These snapshots were examined for every analysis to visually verify expected landslide and wave behavior throughout the calculation. Successively displaying the series of resulting snapshots produces an animation, or movie, of the results that proves to be interesting as well as informative. A CD-ROM has been provided with this report that shows and example of such animation in the form of a Microsoft PowerPoint presentation for Scenario No.1.

Some general observations of interest from inspection of the preceding results include the following points:

- The computed wave amplitudes are consistent with tsunami results measured or estimated for past submarine landslides at various locations, and hence, appear reasonable.

- Results from the LS-TSUN and TUNAMI-N2 programs are generally in good agreement.[9]

- As expected, landslides propagating directly away from the Diablo Canyon site (i.e., with their velocity [and momentum] vector in nearly the same direction as a position vector from the Diablo Canyon site to the landslide's center of mass) – as is substantially the case for Scenarios No. 2, 3, 5, 7, 8, and 9 – produce a leading tsunami wave depression, where the wave first recedes. Landslides propagating directly toward the site – such as for Scenario No. 1 – produce a leading wave high. Scenario No. 13 also has a significant component of its momentum vector directed toward the Diablo Canyon site, and thus also produces a leading wave high. In the cases of Scenarios 4, 6, 10, 11, and 12, the position vectors of the landslides (relative to the Diablo Canyon site) roughly parallel the local shoreline, and the momentum vector of each slide is not too far from being at a right-angle to the position vector. These cases, therefore, produce somewhat intermediate (more complex behavior),

[9] These two programs are representative tools for modeling wave propagation and wave-shore interaction. Use of additional models, based on available methods developed by various experts, can be expected to show considerably

and generally demonstrate a comparatively smaller leading wave depression or high followed by a much more significant wave of opposite polarity.

- The numerical calculations indicate that the site (i.e., the general locale of Sites No. 1 and 2) has little natural protection against locally generated landslide tsunamis. Major wave shoaling occurs as the waves approach the site, and there are no major barriers to reflect or otherwise divert the wave energy as the waves propagate toward the site.

- Wave arrival times vary from about 3 to 27 minutes for the locally generated scenarios considered in this study.

10. Potential Implications of Results

As noted previously, heights of onshore wave run-up at the Diablo Canyon site can be expected to significantly exceed the peak positive amplitudes provided in Table 2. This preliminary study uses a factor of 1.3 to obtain estimates of run-up elevations from the peak positive wave amplitudes provided in Table 2 for Site No. 2. There is considerable uncertainty in this factor, and a more detailed hazard assessment should evaluate such uncertainty. The factor of 1.3 is expected to be lower than a median-centered estimate. Values ranging from 1.0 to over 2.0 are readily supported based on the published literature and variation in expert opinions. For example, in relation to a summary of several methods of run-up calculation, Geist (1999) has stated the following:

> "Despite the accuracy at which tsunami propagation can be modeled, observed run-up values often differ from computed tsunami wave heights by a factor of 2 or more ... The reason for this discrepancy is related particularly to the dynamics of run-up. The consistency between the observed run-up and calculated offshore wave heights has led to the use of an empirical amplification factor to relate modeled tsunamis to run-up values. The amplification factor for wave heights computed at a depth of 50-200 m is usually between 2 and 3, although the factor can range between 1 and 20 depending upon local bathymetric conditions ..."[10]

greater variation in results, and is one component of expert modeling uncertainty. A detailed hazard assessment should adequately evaluate alternative interpretations and associated uncertainties.

[10] In the present study, the water depth at Site No. 1 is 35 m, and so a typical run-up amplification factor relative to wave heights computed at this depth would be somewhat less than the range of 2 to 3 indicated by Geist. If, as a non-conservative approximation, we let a factor 2 correspond to 50 m water depth and a factor of 3 correspond to 200 m water depth, then a run-up factor of 1.9 is obtained relative to wave heights in 35 m water depth. From Table 2, the average amplification factor going from Site 1 to Site 2 is 1.47. Hence, a remaining amplification – i.e., for

Geist's comments are made in the context of earthquake tsunamis, although they derive from studies that consider various types of waves. The situation specifically for landslide tsunamis has been somewhat less studied and can thus be taken as somewhat less understood (with corresponding greater uncertainty). However, it is clear that the run-up amplification factors can be large, and in a detailed hazard assessment run-up factors should be ascertained in consideration of very detailed local elevation data (which, in the case of Diablo Canyon, should include the breakwater and embayment/intake basin, as well as the onshore grades, elevations of buildings, etc.) In this study, however, the subsequent conclusions and recommendations are unaffected even if a minimum run-up factor of 1.0 were to be used.

Using the run-up factor of 1.3, Table 3 provides a summary of impacts of each tsunami wave scenario on some key features pertaining to the Diablo Canyon site. The following observations can be made regarding the expected challenges to Diablo Canyon facilities:

- All 13 scenarios exceed the DCPP design basis for combined peak positive wave amplitude.

- 12 of the 13 scenarios exceed the DCPP design basis for combined peak negative wave amplitude. If combined effects of tsunami, tide, storm surge, and winds are considered (which should be the case when comparing with the design basis combined wave), then all of the 13 scenarios exceed the DCPP design basis for combined peak negative wave amplitude.

- All 13 scenarios produce a wave elevation exceeding the level for which safety components of the auxiliary saltwater (ASW) system are capable of withstanding. All scenarios except perhaps No. 2 and 10 are likely to damage offshore breakwaters and produce a consequent wave draw-down that would cause problems for ASW intake. These scenarios are also likely to lead to debris/sediment clogging of the ASW intake. Resulting loss of ASW intake would be an initiating event for which there is a non-zero risk of core damage (determined as the conditional core damage probability [CCDP] times the likelihood of the initiating event).

- 11 of the 13 scenarios produce run-up also exceeding the main plant grade level at DCPP, and have the potential to damage structures and safety components in the Auxiliary Building, Turbine Building, and other exposed areas of the plant. Some of these damaging scenarios

run-up elevation versus peak positive wave amplitude at Site No. 2 – of about (1.9/1.47)=1.29 would be indicated, which is very close to the factor of 1.3 used in this preliminary study.

would likely produce a level of impairments sufficient to lead directly to core damage (i.e., CCDP=1), whereas others may lead to initiating events having CCDP between 0 and 1.

- 11 of the 13 scenarios produce run-up infringing upon, or inundating, the DC-ISFSI transporter route.

- 2 of the 13 scenarios produce run-up significantly exceeding the elevation of the DC-ISFSI pad. An additional scenario (No. 3) produces run-up that essentially reaches the DC-ISFSI pad level if the design-basis effects of tide, storm surge, and wind waves are superimposed.

Table 3 also provides coarse, judgmental estimates of the repeat time for each scenario based on existing conditions of seismicity, sediment accumulation, etc. These repeat times vary from 750 years to 500,000 years, depending upon the scenario. Lacking further data and evaluation of conditions offshore south-central California, the uncertainty in these estimates is roughly 1 to 2 orders of magnitude, again varying with the scenario. Although such estimates are not considered to be highly reliable and are not sufficient to permit a complete evaluation of tsunami hazard or risk, they can give an indication of the potential importance to risk of landslide tsunamis. As an illustration, given a 50+ m wave striking DCPP (i.e., about 79 ft [24.1 m] above the main plant grade), one would expect that the CCDP would be rather high (if not nearly equal to unity). If even an unrealistically low CCDP of 0.1 is taken for such a scenario, then the core-damage risk contribution from Scenario No. 12 alone would be at least $(0.1)(1/750)\approx 1\times10^{-4}$ per reactor-year. This single scenario would then have a much higher risk contribution than previously expected for all tsunamis. On the other hand, it is possible that further investigation might reveal that the possibility of significant submarine landslides off of Ragged Point is much lower than the estimate, based on judgment, which has been derived in this study.

Without more detailed data (e.g., geological/geophysical parameters, geotechnical parameters, VHR bathymetry), analysis, and expert input, it is therefore difficult to conclude that the existing tsunami design bases of DCPP are adequate and/or that the risk to the site (DCPP and DC-ISFSI) from tsunamis is low.

11. Conclusions and Recommendations

The present study has, based on recent scientific understanding and considerations, identified and analyzed a subset of tsunami scenarios that may affect the Diablo Canyon site. Although this study is preliminary and simplified, it is to our knowledge the most detailed investigation yet undertaken of the landslide tsunami hazard for a specific site along coastal south-central California. Based on current regulatory methods and criteria for developing design bases and evaluating performance of critical facilities, this study has also assessed whether or not the existing bases for tsunami design and performance assessment at the Diablo Canyon site (for DCPP and DC-ISFSI) still appear adequate.

We conclude that the existing tsunami design bases and perceptions of tsunami risk for the Diablo Canyon site no longer reflect modern scientific understanding and methods; there is compelling evidence to suggest that the tsunami threat may be considerably more significant than held in these existing bases and perceptions; and correspondingly, such existing bases and perceptions no longer appear adequate.

Aside from the site-specific analyses performed in this study, similar findings concerning the landslide tsunami threat at other locations have been, and are being, developed by many tsunami scientists. Simultaneously, awareness among the general public of the landslide tsunami threat to coastal cities and facilities has also heightened.

Furthermore, there is reason to believe that challenges to tsunami design bases and risk perceptions are not unique to the Diablo Canyon site, but are likely applicable on a generic basis to all coastal nuclear facilities.

In consideration of these factors and the specific findings produced in this study, we make the following recommendations:

1. Arrange a meeting to discuss this study, its findings/recommendations, and the potential implications to Diablo Canyon and other nuclear facilities.

2. Prepare preliminary regulatory guidance on evaluation and review for state-of-the-art tsunami hazard assessment and its use. The guidance should include the following components:

    - A screening methodology for all tsunamigenic sources;

- To address the tsunamigenic sources that cannot be screened out, a description of probabilistic hazard analysis methods for determining the annual exceedance frequencies and return periods of site wave effects (needed to evaluate design bases, and implement risk assessment and risk-informed regulation), and for determining the characteristics of controlling tsunami scenarios.

- A description of deterministic hazard analysis methods for detailed analysis of the wave effects for the controlling tsunami scenarios.

- A description of the various types and quality of data, field investigations, and scientific input needed for state-of-the-art implementation of tsunami hazard assessment.

- A description of the methods for analysis of uncertainties including alternative interpretation of experts (which may, for example, be similar to guidance already in place for earthquake hazard assessment).

- A description on the use of tsunami hazard results in developing or evaluating tsunami design bases and in assessing facility performance/risk.

3. Perform preliminary tsunami hazard assessments and review evaluations of the tsunami design bases at a sample of other coastal nuclear power facilities, as a basis for ascertaining whether or not tsunami design-basis adequacy may be a generic issue. Locations on the Pacific, Gulf, and Atlantic Coasts should be included in the sample to gain insights into regional severity/characteristics of tsunami hazard.

4. Sponsor scientific workshops on tsunami hazard assessment for U.S. coastal nuclear power plants and critical facilities, and obtain information useful for deciding on subsequent action, if any. Also, seek comments on the preliminary regulatory guidance and preliminary hazard assessments derived, respectively, from the preceding recommendations.

5. In accordance with any need for further action that may be suggested from the preceding activities, develop a regulatory program for site screening and safety evaluation (including tsunami hazard and risk assessment, as warranted) for U.S. nuclear facilities.

6. Aside from the foregoing items, for the Diablo Canyon site request the licensee to justify and/or re-evaluate the tsunami design bases and perform a state-of-the-art assessment of tsunami hazard and risk (including DCPP and DC-ISFSI) within the umbrella of its existing long-term seismic program (LTSP).

12. List of Cited and/or Relevant References

Bohannon, R.G., and J.V. Gardner (2003). "Submarine landslides of San Pedro Sea Valley, southwest of Long Beach, California." *Marine Geology* (in press).

California Coastal Commission (2002). Letter to Secretary, U.S. Nuclear Regulatory Commission. October 16.

California Department of Fish and Game [CDFG], Information Technology Branch (2003). "California Department of Fish and Game (DFG) Spatial Data Resources; Bathymetry Project, Second Edition," http://maphost.dfg.ca.gov/bathymetry.htm.

California Spatial Information Library [CaSIL] (2000). http://www.gis.ca.gov/.

Day, S.J., J.C. Carracedo, H. Guillou, and P. Gravestock (1999). "Recent structural evolution of the Cumbre Vieja volcano, La Palma, Canary Islands: volcanic rift zone reconfiguration as a precursor to volcano flank instability?" *Journal of Volcanology and Geothermal Research,* Vol. 94, pp. 135-167. Elsevier.

Eisner, R.K. (2001). "State of California tsunami 5-year review (1997-2001)," ITS 2001 Proceedings, NTHMP Review Session, Paper R-13. International Tsunami Society.

Fritz, H.M. (2000). "Initial phase of landslide generated impulse waves," Mitteilungen 178, Versuchsanstalt für Wasserbau, Hydrologie und Glaziologie der Eidgenössischen, Technischen Hochschule Zürich.

Fryer, G.J., P. Watts, and L.F. Pratson (2003). "Source of the tsunami of 1 April 1946: A landslide in the upper Aleutian forearc." *Marine Geology* (in press).

Geist, E. L. (2000). "Origin of the 17 July 1998 Papua New Guinea Tsunami: earthquake or landslide." *Seismological Research Letters*, Vol. 71, pp. 344-351.

Geist, E. L. (1999b). "Descriptive Model of the July 17, 1998 Papua New Guinea Tsunami," http://walrus.wr.usgs.gov/tsunami/specs.html.

Geist, E. L. (1999a). "Local Tsunamis and Earthquake Source Parameters," *in Tsunamigenic Earthquakes and Their Consequences*, Advances in Geophysics (Edited by Renata Dmowska and Barry Saltzman), Volume 39, Academic Press.

Goldfinger, C., L.D. Kulm, L.C. McNeill, and P. Watts (2000). "Super-scale failure of the southern Oregon Cascadia margin," *Pure and Applied Geophysics*, Vol. 157, pp. 1189-1226. Birkhäuser Verlag, Basel.

González, F.I. (May 1999). "Tsunami," *Scientific American*, Vol. 280, No. 5, pp. 56-65.

Grilli, S. T., S. Vogelmann, and P. Watts (2002). "Development of a 3D numerical wave tank for modeling tsunami generation by underwater landslides," *Engineering Analysis with Boundary Elements*, Vol. 26, pp. 301-313, Elsevier.

Grilli, S.T., I. A. Svendsen, and R. Subramanya (1997). "Breaking Criterion and Characteristics for Solitary Waves on Slopes," *ASCE Journal of Waterway, Port, Coastal, and Ocean Engineering*, May/June Vol., p. 102.

Hemphill-Haley, E., and R. C. Lewis (2003), "Diatom Data From Bradley Lake, Oregon: Downcore Analyses," U.S. Geological Survey Open-File Report 03-190.

Hwang, L., et al. (September 1974). "Earthquake Generated Water Waves at the Diablo Canyon Power Plant". (Appendix D of Appendix 2.4C to Diablo Canyon Power Plant Final Safety Analysis Report as amended through August 1980). Tetra Tech Report No. TC-443, Tetra Tech Incorporated, Pasadena, CA.

Hwang, L., A. F. H. Yuen, and M. Brandsma (March 1975). "Earthquake Generated Water Waves at the Diablo Canyon Power Plant, (Part Two)." (Appendix E of Appendix 2.4C to Diablo Canyon Power Plant Final Safety Analysis Report as amended through August 1980). Tetra Tech Report No. TC-443B, Tetra Tech Incorporated, Pasadena, CA.

Johnson, J.M. (1999). "Heterogeneous Coupling along Alaska-Aleutians as Inferred from Tsunami, Seismic, and Geodetic Inversions," *in Tsunamigenic Earthquakes and Their Consequences,* Advances in Geophysics (Edited by Renata Dmowska and Barry Saltzman), Volume 39, Academic Press.

Johnson, C., and C.L. Mader. (1994). "Modeling the 105 Ka Landslide Lanai Tsunami," *Science of Tsunami Hazards*, Vol. 12, p. 3.

Lee, H.J., R.E. Kayen, J.V. Gardner, and J. Locat (2003). "Characteristics of several tsunamigenic submarine landslides," in Submarine Mass Movements and Their Consequences, J. Locat and J. Mienert (editors), pp. 357-366. Kluwer Academic Publishers, The Netherlands.

Lee, H.J., J.P.M. Syvitski, G. Parker, D. Orange, J. Locat, E.W.H. Hutton, and J. Imran (2002). "Distinguishing sediment waves from slope failure deposits: field examples, including the 'Humboldt slide', and modeling results," *Marine Geology*, Vol. 192, pp. 79-104.

Lee, H. J. (2002), "Factors Influencing Occurrence, Scale, Mobility, Runout, and Morphology of Mass Movements on the Continental Slope," http://marine.usgs.gov.

Legg, M. R., J. C. Borrero, and C. E. Synolakis (January 2003). "Evaluation of Tsunami Risk to Southern California Coastal Cities," The 2002 NEHRP Professional Fellowship Report, Earthquake Engineering Research Institute (EERI).

Legg, M.R., and M. J. Kamerling (2002). "Large-scale basement-involved landslides along the California continental borderland."

Lynett, P., and P. L.-F. Liu (2002). "A numerical study of submarine-landslide-generated waves and run-up," *Proceeding of the Royal Society*, Vol. 458, pp. 2885-2910, London.

Mader, C.L. (1997). "Modeling the 1994 Skagway Tsunami," Science of Tsunami Hazards, Vol. 15, p. 41.

Mader, C.L. (1990). "Numerical Tsunami Flooding Study - I," *Science of Tsunami Hazards*, Vol. 8, p. 67.

Mader, C.L. (1988). *Numerical Modeling of Water Waves*, Los Alamos Series in Basic and Applied Sciences, University of California Press, Berkeley and Los Angeles, California.

Mader, C.L. (1984). "A Landslide Model for the 1975 Hawaii Tsunami," *Science of Tsunami Hazards*, Vol. 2, p. 71.

Mader, C.L., D.W. Moore, and G.F. Carrier (1993a). "Numerical Tsunami Source Study - II," *Science of Tsunami Hazards*, Vol. 11, p. 81.

Mader, C.L., D.W. Moore, and G.F. Carrier (1993b). "Numerical Tsunami Propagation Study - III," *Science of Tsunami Hazards*, Vol. 11, p. 93.

McAdoo, B.G., and P. Watts (2000). "Tsunami hazard from submarine landslides on the Oregon continental slope." *Marine Geology* (in press).

NEES (2003). "Chapter 2. Issues in Earthquake Engineering Research; Subsection: Tsunamis in waiting."

National Fire Protection Association [NFPA] (1994). "Standard for the Production, Storage, and Handling of Liquefied Natural Gas (LNG)," NFPA 59A, 1994 Ed.

Pararas-Carayannis, G. (2001) "Subject: Re: Tsunami threats to coastal nuclear power plants," Email correspondence to Russell D. Hoffman. June 26. Internet site: http://www.animatedsoftware.com/environm/onofre/pararas1.htm

Pelinovsky, E.N., and Mazova, R. Kh. (1992). "Exact Analytical Solutions of Nonlinear Problems of Tsunami Wave Run-up on Slopes with Different Profiles," Natural Hazards, Vol. 6, p. 227-249.

Pacific Gas & Electric [PG&E] Company (2002b). "Response to: Request For Additional Information for the Diablo Canyon Independent Spent Fuel Storage Installation Application (TAC No. L23399)," PG&E Letter DIL-02-009 to USNRC.

PG&E (2002a). "Diablo Canyon Independent Spent Fuel Storage Installation (ISFSI) Safety Evaluation Report," submitted to U.S. Nuclear Regulatory Commission (USNRC) as part of license application.

PG&E (2001). "Diablo Canyon Power Plant (DCPP) Units 1 & 2 Final Safety Analysis Report (FSAR) Update, Revision 14, November 2001." submitted to U.S. Nuclear Regulatory Commission (USNRC) as part of licensing commitment.

PG&E (July 1988). "Final Report of the Diablo Canyon Long Term Seismic Program." Docket Nos. 50-275 and 50-323, submitted to U.S. Nuclear Regulatory Commission (USNRC) as part of licensing condition.

Pure and Applied Geophysics (2003). Special volume on landslide tsunamis, edited by J. P. Bardet, C. E. Synolakis, H. L. Davies, F. Imamura, E. A. Okal, with papers from the workshop on "The Prediction of Underwater Landslide and Slump Occurrence and Tsunami Hazards off of Southern California," *Pure and Applied Geophysics,* Vol. 160, No. 10-11, 2003. http://www.birkhauser.ch/journals/2400/2400_160_10-11.htm.

Sandwell, D. and W.H.F. Smith, (1996). "Global Bathymetric Prediction for Ocean Modeling and Marine Geophysics," http://topex.ucsd.edu/marine_topo/mar_topo.html.

Sandwell, D.T., W.H.F. Smith, S.M. Smith, and C. Small, "Measured and Estimated Seafloor Topography," Internet sites: http://topex.ucsd.edu/marine_topo/mar_topo.html, and http://topex.ucsd.edu/cgi-bin/get_data.cgi.

Santa Barbara News-Press (May 11, 2003). "Tsunami threat hangs over cliffs; scientists say underwater landslides could trigger the big waves off the Goleta coast."

Satake, K. (2001) "Tsunami modeling from submarine landslides," ITS 2001 Proceedings, Session 6, Number 6-4. International Tsunami Society.

Sewell, R.T. (May 2003). "On the Science-Engineering Interface; The Practical Viewpoint in Benchmarking and Validation of Landslide Tsunami Models." In abstract-proceedings and presentation at the *Workshop on Model Validation and Benchmarking for Tsunami Generation by Submarine Mass Failure*; May 30-31, 2003; Honolulu, Hawaii; sponsored by The National Science Foundation (NSF) and CMS-Geomechanics and Geotechnical Systems.

Sewell, R.T. (December 13, 2002). "Tsunami hazard and design bases; specific issues for the Diablo Canyon site and implicit generic issues for existing coastal nuclear facilities," R.T. Sewell Associates, Consulting, Technical Note to J. Stamatakos of Southwest Research Institute.

Sewell, R.T. (November 20, 2002). "Review of Diablo Canyon (DC) Independent Spent Fuel Storage Installation (ISFSI) Safety Analysis Report (SAR), Section 2.4.6 'Probable Maximum Tsunami Flooding'," R.T. Sewell Associates, Consulting, Technical Memo to J. Stamatakos of Southwest Research Institute.

Sewell, R.T. (May 2002). "Probabilistic tsunami hazard and risk assessment." In abstract-proceedings and presentation at the *Second International Tsunami Symposium*; May 28-30, 2002; Honolulu, Hawaii; sponsored by The Tsunami Society.

Tadepalli, S., and Synolakis, C.E. (1994). "The Run-Up of N-Waves on Sloping Beaches," *Proceedings of the Royal Society of London*, Vol. A 445, pp. 99-112.

Tappin, D.R., P. Watts, and T. Matsumoto (2003). "Architecture and Failure Mechanism of the Offshore Slump Responsible for the 1998 Papua New Guinea Tsunami," in Submarine Mass Movements and Their Consequences, J. Locat and J. Mienert (Eds.), Kluwer Academic Publishers, Dordrecht, 383-389, 2003.

Tappin, D.R., P. Watts, G.M. McMurty, Y. Lafoy, and T. Matsumoto (2001). "The Sissano, Papua New Guinea tsunami of July 1998 – offshore evidence on the source mechanism," *Marine Geology*, Vol. 175, pp. 1-23.

Tetra Tech, Inc. (July 1976). "User's Guide to Seawave: A Model of Tsunami Generation and Propagation," Authored by M. Brandsma, D. Divoky, and L. Hwang.

Titov, V.V., and F.I. Gonzãlez (November 1997). "Implementation and Testing of the Method of Splitting Tsunami (MOST) Model," *NOAA Technical Memorandum ERL PMEL-112*, National Oceanic and Atmospheric Administration, Contribution No. 1927 from NOAA/Pacific Marine Environmental Laboratory.

USGS EROS Data Center, NASA Distributed Active Archive Center. "GTOPO30 Land Topography," Internet sites: http://edcdaac.usgs.gov/gtopo30/gtopo30.html, and http://edcdaac.usgs.gov/gtopo30/e100n40.html.

USNRC (2002). "Request For Additional Information for the Diablo Canyon Independent Spent Fuel Storage Installation Application (TAC No. L23399)," letter from J.R. Hall (USNRC) to L.F. Womack (DCPP). August 29.

USNRC (2001). "Draft Regulator Guide DG-1110: An Approach for Using Probabilistic Risk Assessment in Risk-Informed Decisions on Plant-Specific Changes to the Licensing Basis," Proposed revision 1 to R.G. 1.174, June.

USNRC (2000). "Standard Review Plan for Spent Fuel Dry Storage Facilities," NUREG-1567, March.

USNRC (1997). "Regulatory Guide 1.165 - Identification and Characterization of Seismic Sources and Determination of Safe Shutdown Earthquake Ground Motion," March.

USNRC (1991), "Procedure and Submittal Guidance for the Individual Plant Examination of External Events (IPEEE) for Severe Accident Vulnerabilities," U. S. Nuclear Regulatory Commission, NUREG-1407, May.

Von Huene, R., C.R. Ranero, and P. Watts (2003). "Tsunamigenic slope failure along the Middle America Trench in two tectonic settings." *Marine Geology* (in press).

Ward, S.N., and S. Day (2002). "Ritter Island Volcano - Lateral collapse and tsunami of 1888," *Geophysical Journal International* (in press).

Ward, S.N., and S. Day (2002). "Cumbre Vieja Volcano -- Potential collapse and tsunami at La Palma, Canary Islands," *Geophysical Research Letters*, Vol. 28, p.397-400.

Watts, P. (November 19, 2003). personal communication.

Watts, P. (2003). "Probabilistic Analyses of Landslide Tsunami Hazards," in Submarine Mass Movements and Their Consequences, J. Locat and J. Mienert (Eds.), Kluwer Academic Publishers, Dordrecht, 163-170, 2003.

Watts, P., S. T. Grilli, J. T. Kirby, G. J. Fryer, and D. R. Tappin (2003). "Landslide tsunami case studies using a Boussinesq model and a fully nonlinear tsunami generation model," *Natural Hazards and Earth System Sciences*, Vol. 3, pp. 391–402, European Geosciences Union.

Watts, P. (2002b). "Probabilistic predictions of landslide tsunamis off southern California," *Marine Geology* (in press).

Watts, P. (2002a). "Los Angeles and Long Beach harbor response to local tsunami attack," submitted in 2002 to ASCE Journal of *Waterway, Port, Coastal, and Ocean Engineering* by Applied Fluids Engineering, Inc., Long Beach, CA.

Watts, P. (2001). "Some Opportunities of the Landslide Tsunami Hypothesis," *Science Of Tsunami Hazards*, Vol. 19(3), pp. 126-149.

Wessel, P., and W.H.F. Smith (October 2000). "The Generic Mapping Tools, GMT, Version 3.3.6," School of Ocean and Earth Science and Technology, University of Hawaii at Manoa.

Wiegel, R. L. (1970). "Tsunamis," Chapter 11 in *Earthquake Engineering*, Robert L. Wiegel, Coordinating Editor, Prentice-Hall, Inc., Englewood Cliffs, N.J.

Wilson, B. W. (October 1974). "Estimate of Tsunami Effect at Diablo Canyon Nuclear Generating Station, California," report to Pacific Gas and Electric Company by Basil W. Wilson D.Sc., Consulting Oceanographic Engineer, Pasadena, CA.

Table 1 Characteristics of the Submarine Landslides Used for Tsunami Scenario Analysis

Scenario No.[1]	Area (km^2)	Volume (km^3)	Average Height (m)	Peak Height (m)	Travel Distance (km)	Average Velocity (m/s)
1	172.	7.56	44.	79.	10.0	25.0
2	118.	3.18	27.	63.	6.00	17.5
3	494.	109.	221.	564.	11.3	60.0
4	279.	153.	548.	820.	31.6	75.0
5	262.	73.2	279.	625.	26.1	45.0
6	617.	66.2	107.	233.	36.9	60.0
7	1580.	1100.	696.	1450.	36.9	50.0
8	951.	273.	287.	838.	17.2	25.0
9	1760.	1080.	614.	1280.	13.5	15.0
10	86.	1.88	22.	105.	10.8	25.0
11	517.	57.3	111.	316.	24.2	35.0
12	172.	15.6	91.	338.	17.5	40.0
13	786.	381.	485.	876.	18.4	60.0

[1] Actual order that these scenarios were analyzed in this study: 1, 2, 3, 4, 5, 6, 7, 13, 12, 9, 8, 10, and 11.

Table 2 Peak Wave Amplitudes from Tsunami Analysis of the 13 Landslide Scenarios

SITE 1 (APPROXIMATELY 1 KM OFFSHORE DIABLO CANYON)													
Peak Positive Wave Amplitude (m), for Scenario:													
	1	2	3	4	5	6	7	8	9	10	11	12	13
LS-TSUN	+14.9	+7.7	+55.2	+25.1	+15.4	+23.7	+127.	+22.7	+32.4	+4.8	+28.4	+28.6	+114
TUNAMI-N2	+13.8	+8.2	+44.4	+25.5	+15.3	+23.4	--	+21.1	+19.1	+4.7	+26.6	+22.2	+85.1.
Peak Negative Wave Amplitude (m), for Scenario:													
	1	2	3	4	5	6	7	8	9	10	11	12	13
LS-TSUN	-15.7	-6.7	BOT	BOT	-17.7	-25.6	BOT	-28.2	BOT	-3.8	BOT	BOT	BOT
TUNAMI-N2	-16.0	-6.0	BOT	BOT	-17.9	-25.4	--	-29.4	BOT	-4.1	BOT	-29.3	BOT
SITE 2 (AT DIABLO CANYON SHORE)													
Peak Positive Wave Amplitude (m), for Scenario:													
	1	2	3	4	5	6	7	8	9	10	11	12	13
LS-TSUN	+25.4	+11.3	+69.6	+40.8	+25.8	+24.0	+167.	+27.8	+33.4	+11.6	+48.6	+45.2	+132.
TUNAMI-N2	+21.5	+9.4	+57.0	+37.9	+28.5	+29.7	--	+25.2	+25.1	+10.0	+37.6	+36.7	+111.
Peak Negative Wave Amplitude (m), for Scenario:													
	1	2	3	4	5	6	7	8	9	10	11	12	13
LS-TSUN	BOT	BOT	BOT	BOT	BOT	BOT	BOT	BOT	BOT	-2.5	BOT	BOT	BOT
TUNAMI-N2	BOT	BOT	BOT	BOT	BOT	BOT	--	BOT	BOT	-2.3	BOT	BOT	BOT

Notes: 1. "BOT" indicates that the wave has bottomed-out at this location, meaning that it has receded below this level.
2. Due to the limited grid coverage, and the fact that input to TUNAMI-N2 is developed as the wave configuration determined from LS-TSUN at the time the landslide movement is complete, TUNAMI-N2 wave amplitudes could not be obtained for Scenario No. 7.

Table 3 Impacts on the Diablo Canyon Site of the 13 Landslide Scenarios

	Scenario												
No.	1	2	3	4	5	6	7	8	9	10	11	12	13
Estimated Repeat Time [1] (ky)	7.5	15.	10.	5.	5.	5.	500.	50.	100.	1.5	2.5	0.75	50.
Diablo Canyon Feature	**Site Challenge Impact Matrix[2]**												
Design Basis: Peak Positive Wave Amplitude; +32 ft [+9.8 m] MSL	yes	yes	yes	yes	yes	yes	yes	yes	yes	yes	yes	yes	yes
Design Basis: Peak Negative Wave Amplitude; –11.6 ft [-3.5 m] MSL	yes	yes	yes	yes	yes	yes	yes	yes	yes	no	yes	yes	yes
ASW Safety Components El. +45.4 ft [+13.8 m] MSL	yes	yes	yes	yes	yes	yes	yes	yes	yes	yes	yes	yes	yes
DCPP Main Plant Grade El. +85 ft [+25.9 m] MSL	yes	no	yes	yes	yes	yes	yes	yes	yes	no	yes	yes	yes
DC-ISFSI Transporter Route El. +80 ft [+24.4 m] MSL	yes	no	yes	yes	yes	yes	yes	yes	yes	no	yes	yes	yes
DC-ISFSI Pad El. +310 ft [+94.5 m] MSL	no	no	no	no	no	no	yes	no	no	no	no	no	yes

[1]Repeat times are coarse estimates based on judgment, and they can be taken as central estimates within a range having roughly a 1 to 2 order of magnitude variation. Judgments concerning repeat times have been made considering seismic activity and potential, apparent degree of sediment accumulation, local gradient, evidence of past slumping/sliding, similarity or dissimilarity to past events and their repeat times, and other factors. The repeat times apply to each specific scenario (landslide and wave produced), assume conditions (seismicity, sediment accumulation, etc.) as they presently are, and are not return periods for wave effects at the site. Assessment of return periods for wave effects at a specific site requires probabilistic synthesis of a reasonably comprehensive set of scenarios, their site effects, and their likelihoods. In addition, for final hazard assessment, input from marine geologists and other experts should be obtained considering all applicable data, with at least one objective being to refine the estimates of scenario repeat times.

[2] Impacts from the tsunami wave only; this matrix does not consider the superimposition of tides, storm surge, and wind-induced waves on the scenario tsunami waves, however, the Diablo Canyon design basis values (as noted in this table)

C01

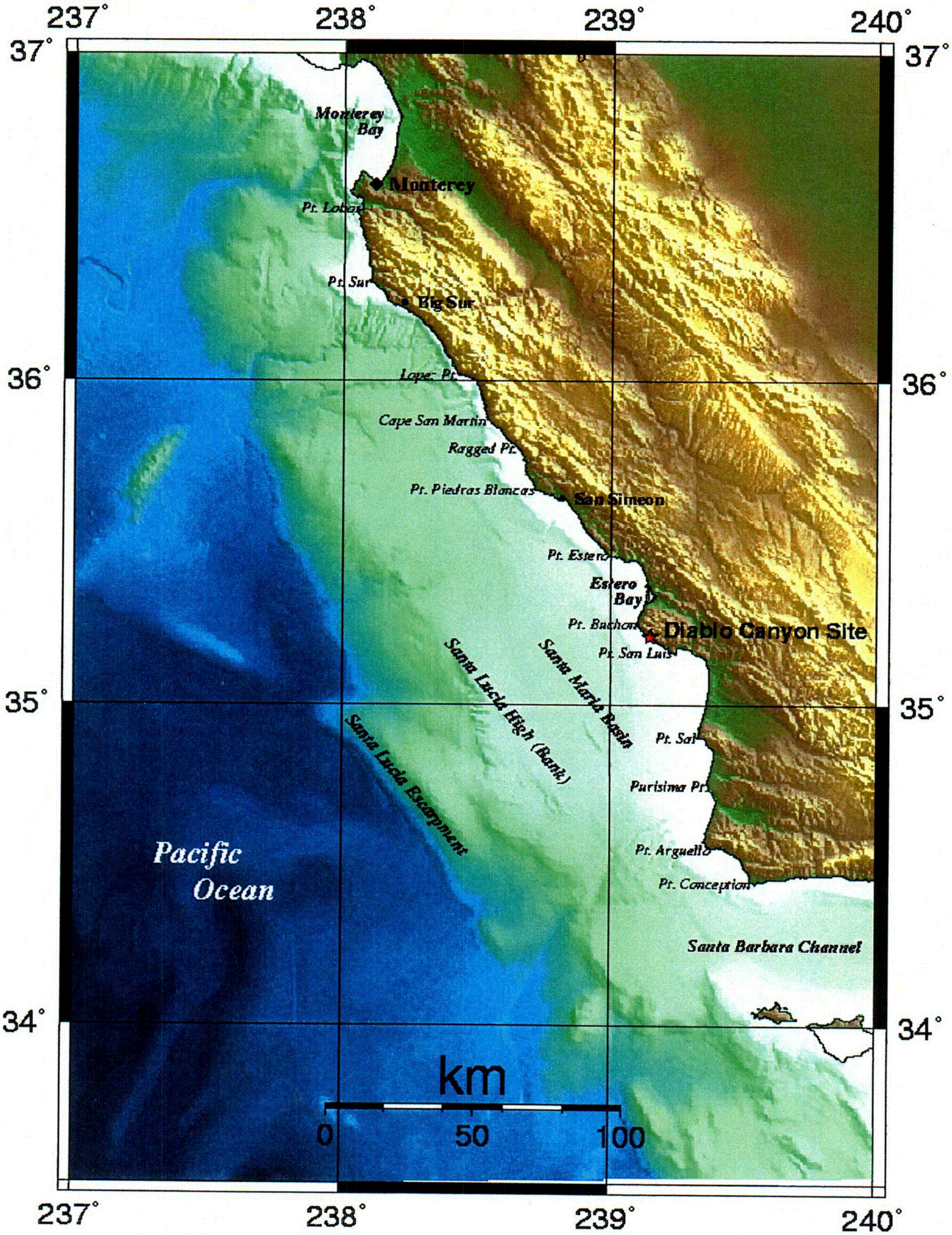

Figure 1 Color image of study region as view from above, showing locations of interest. (Illumination source is in the northeast.)

C02

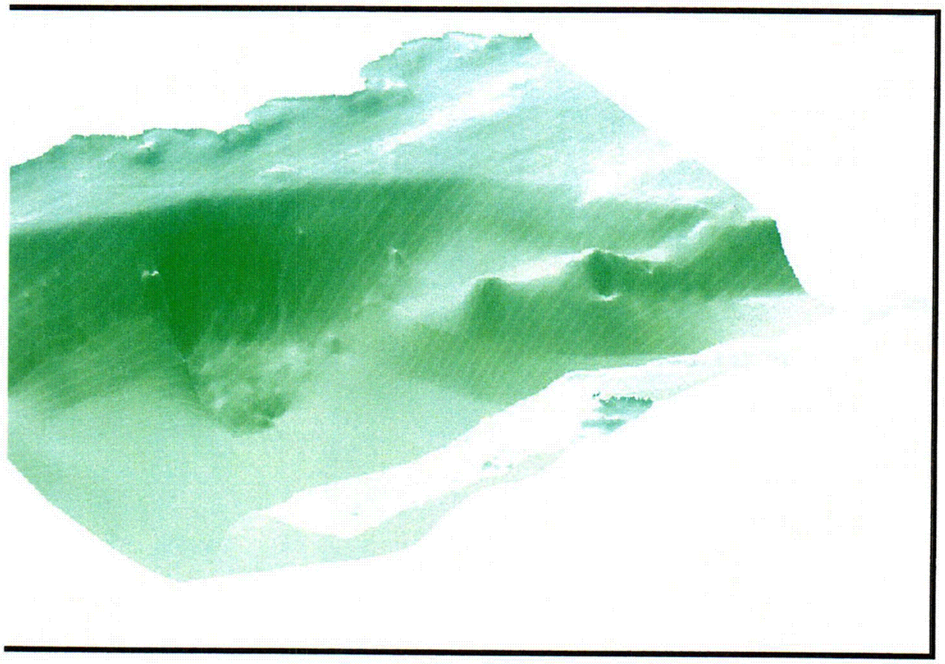

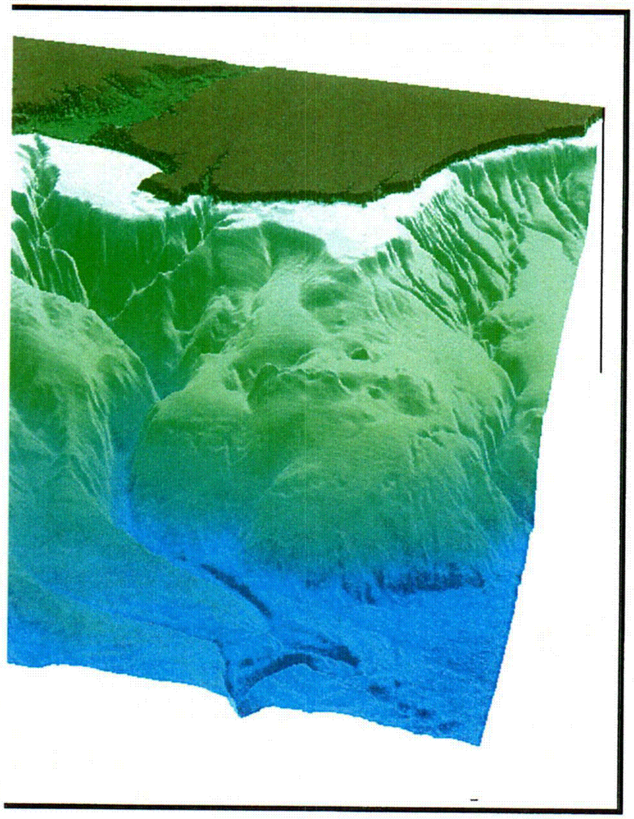

Figure 2 Examples of past significant slides evident from bathymetry images; Goleta slide within Santa Barbara Channel (top), and slide off of Pt. Sur / Pt. Lobos (bottom).

C03

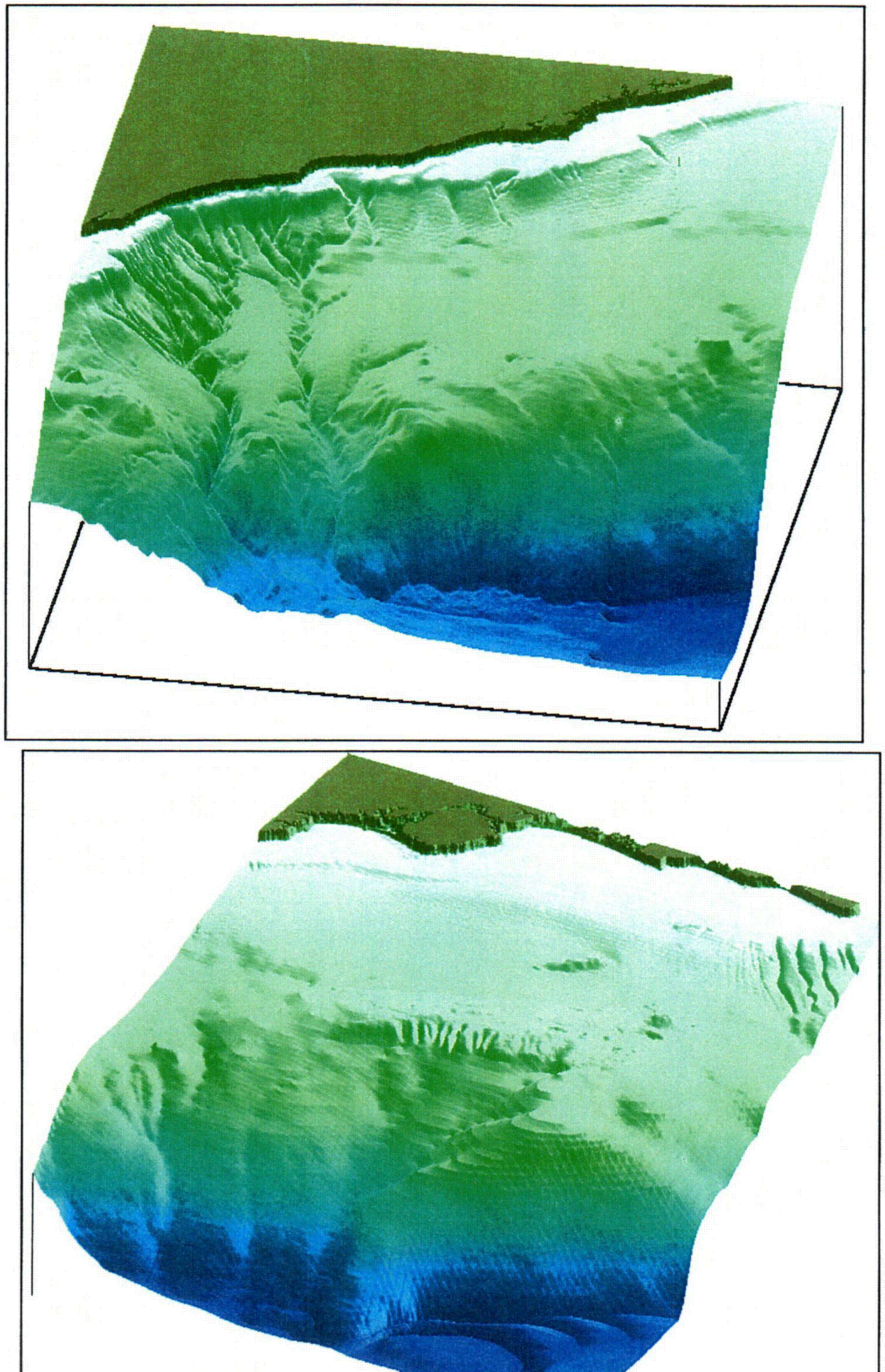

Figure 3 Bathymetry images covering the study region; Point.Sur to Point Piedras Blancas (left), and Point Estero to Point Arguello (right).

C04

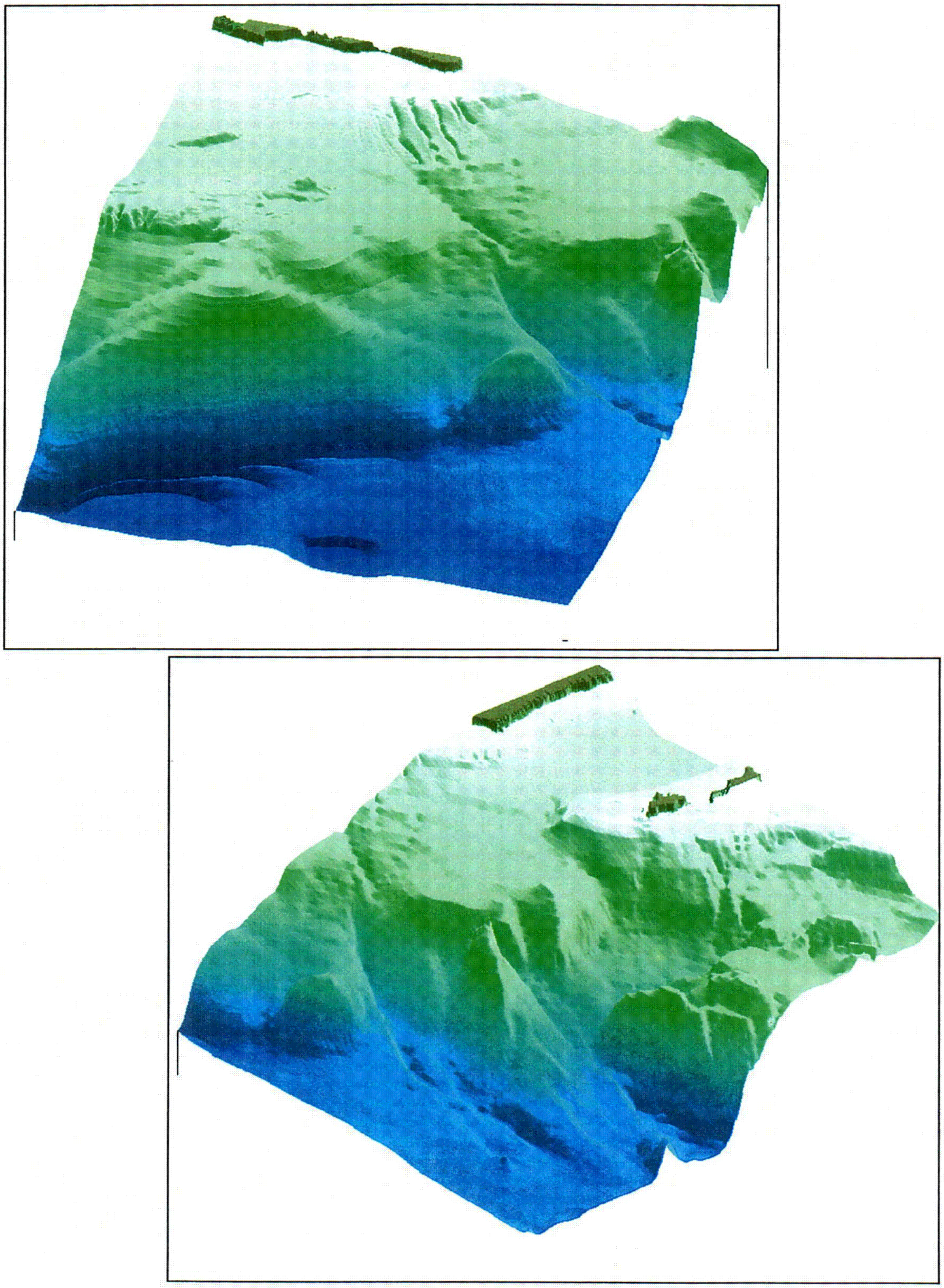

Figure 4 Bathymetry images covering the study region; Point.Sal to Point Conception (top), and the offshore vicinity at the mouth of the Santa Barbara Channel (bottom).

C05

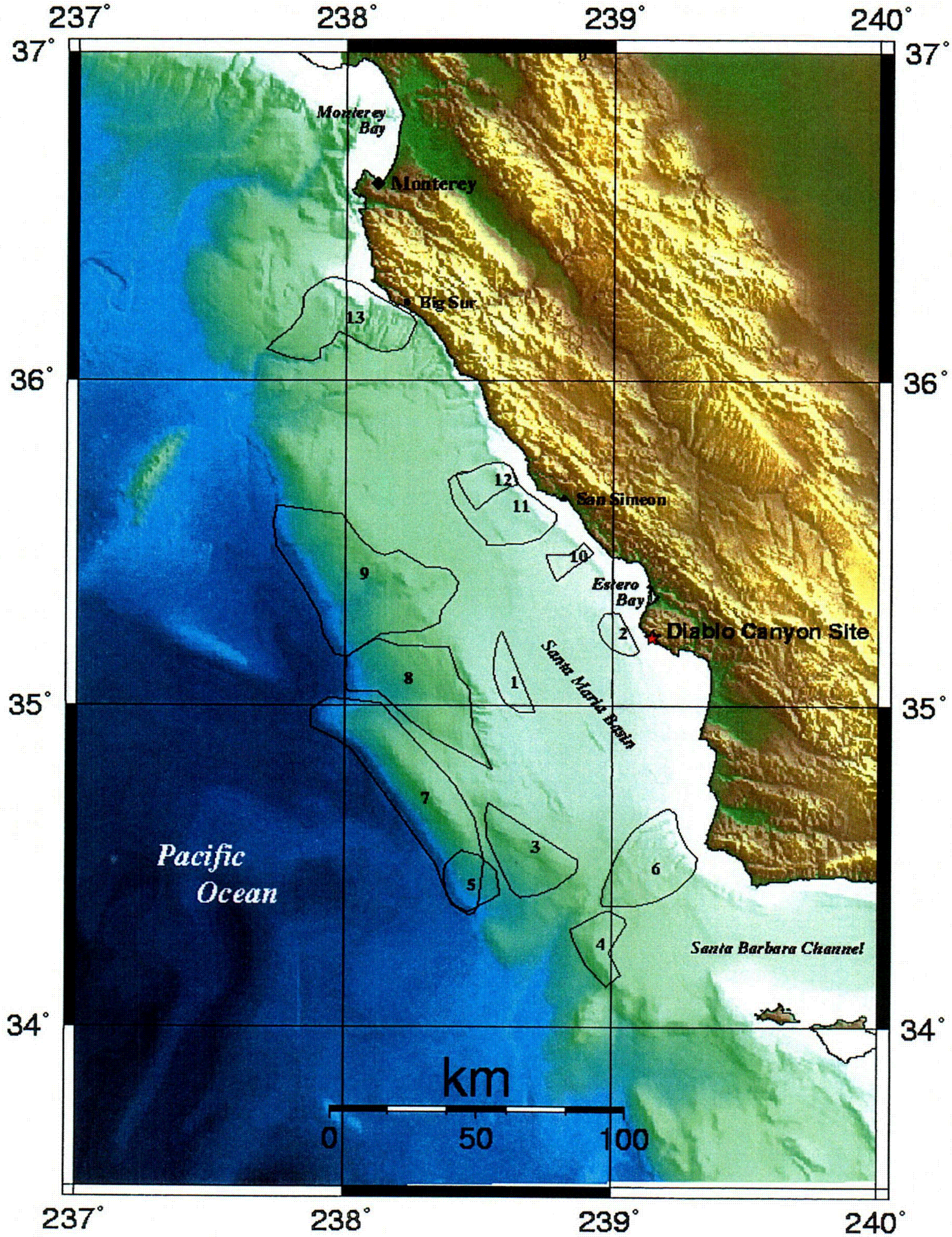

Figure 5 Outline of areas for the landslide scenarios identified and selected for this study. (Illumination source is in the northeast.)

C06

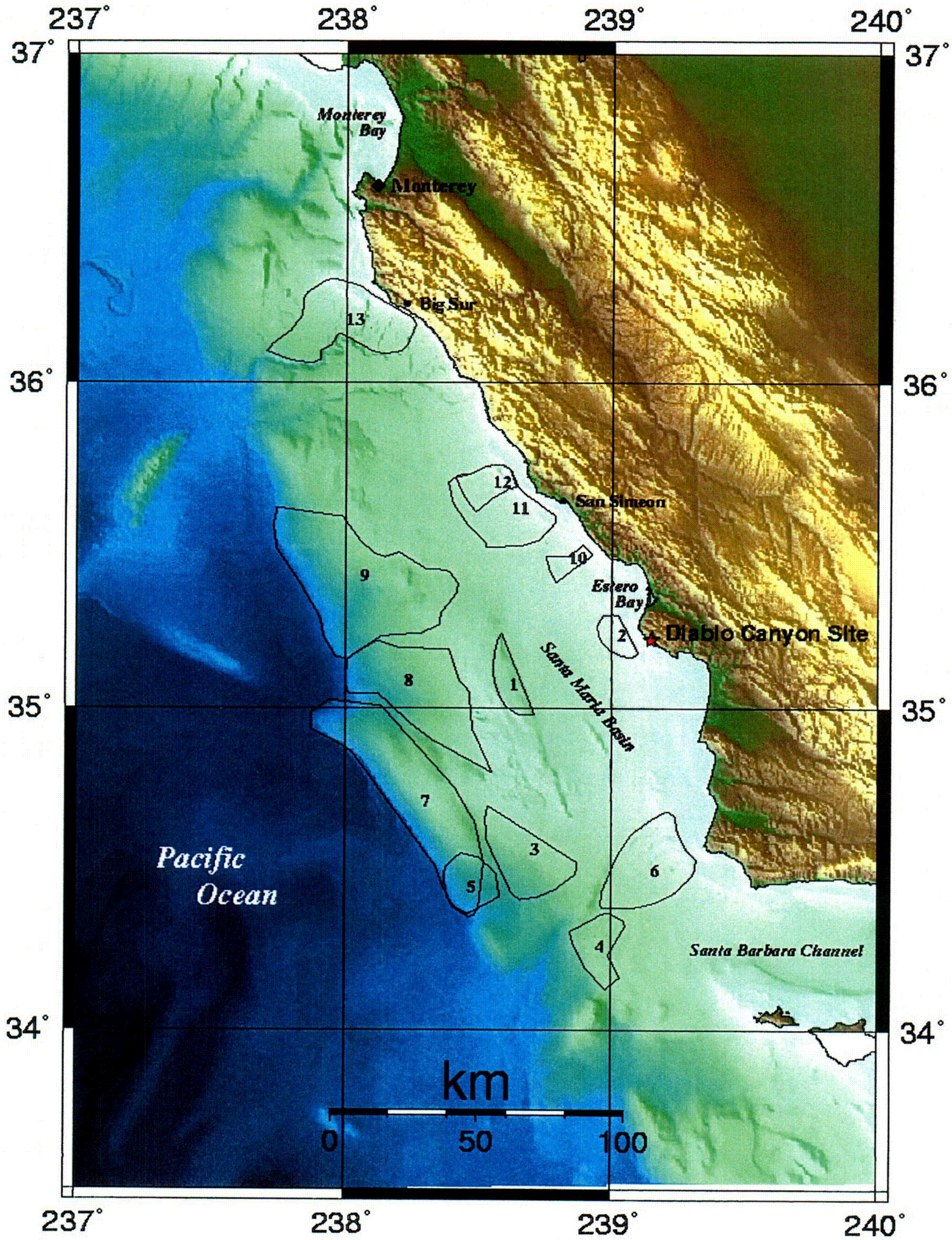

Figure 6 Outline of areas for the landslide scenarios identified and selected for this study. (Illumination source is in the southwest. Note the visibility of Santa Lucia High.)

C07

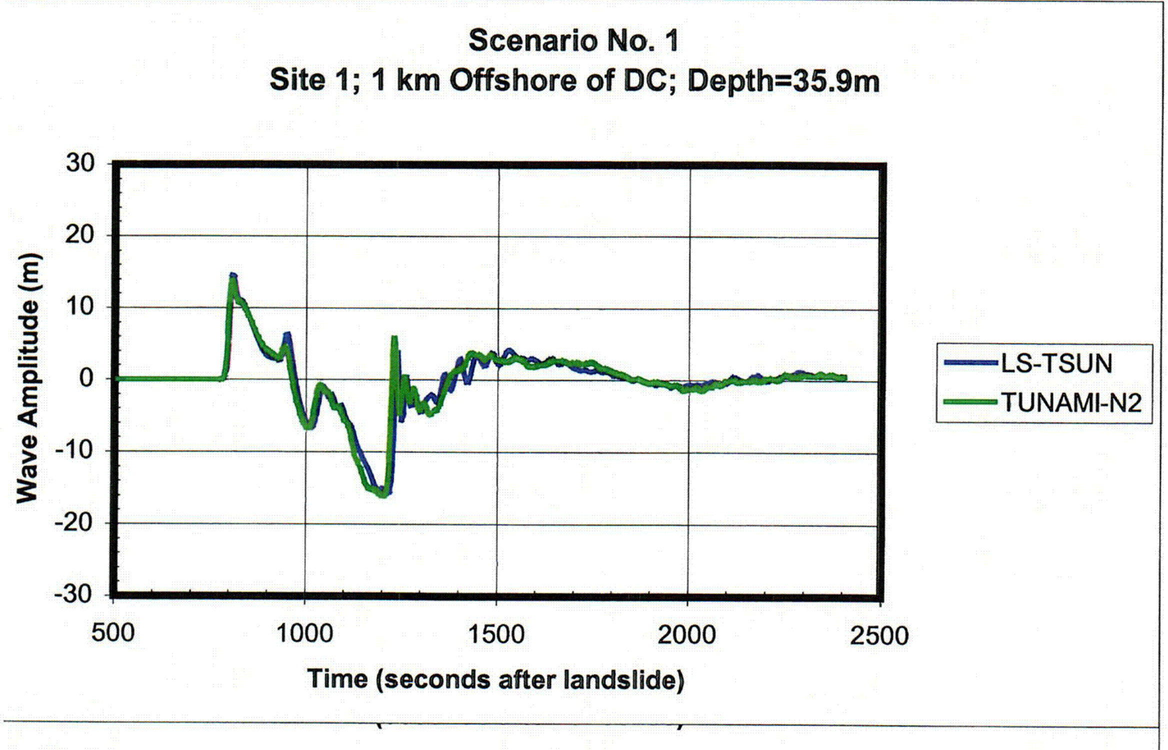

Figure 7 Wave amplitude time histories at Site 1 (above) and Site 2 (below) for Landslide Scenario No. 1.

C08

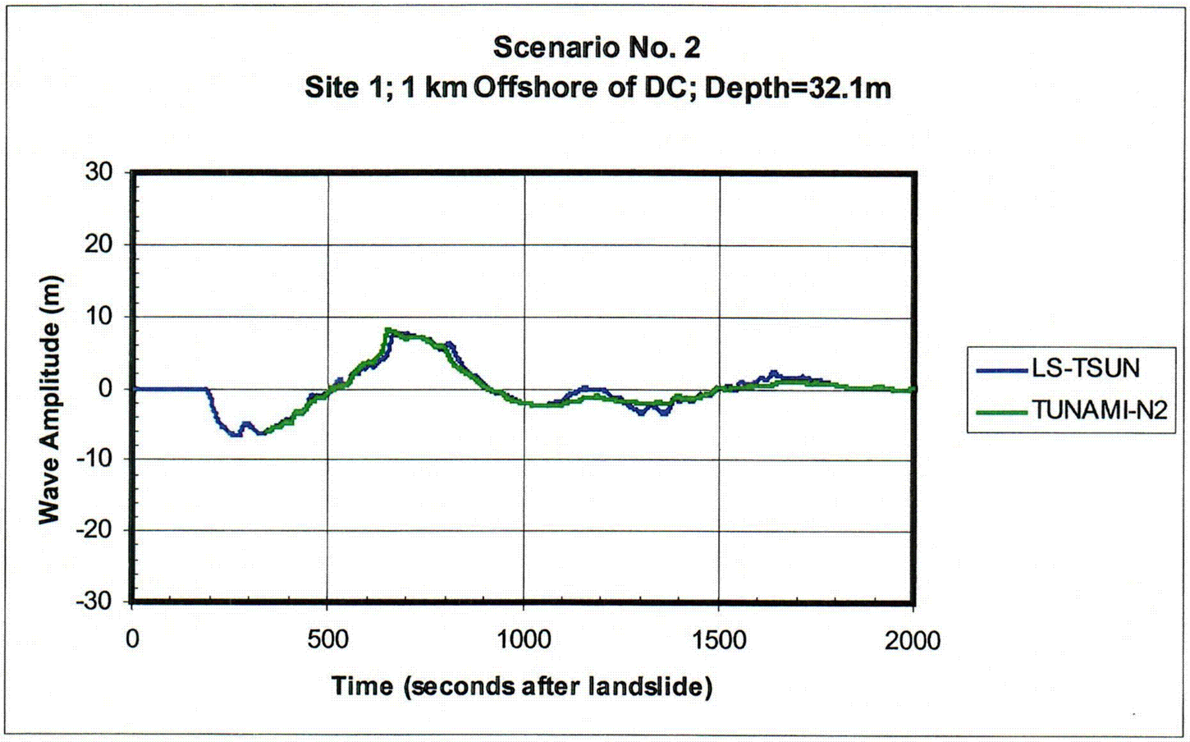

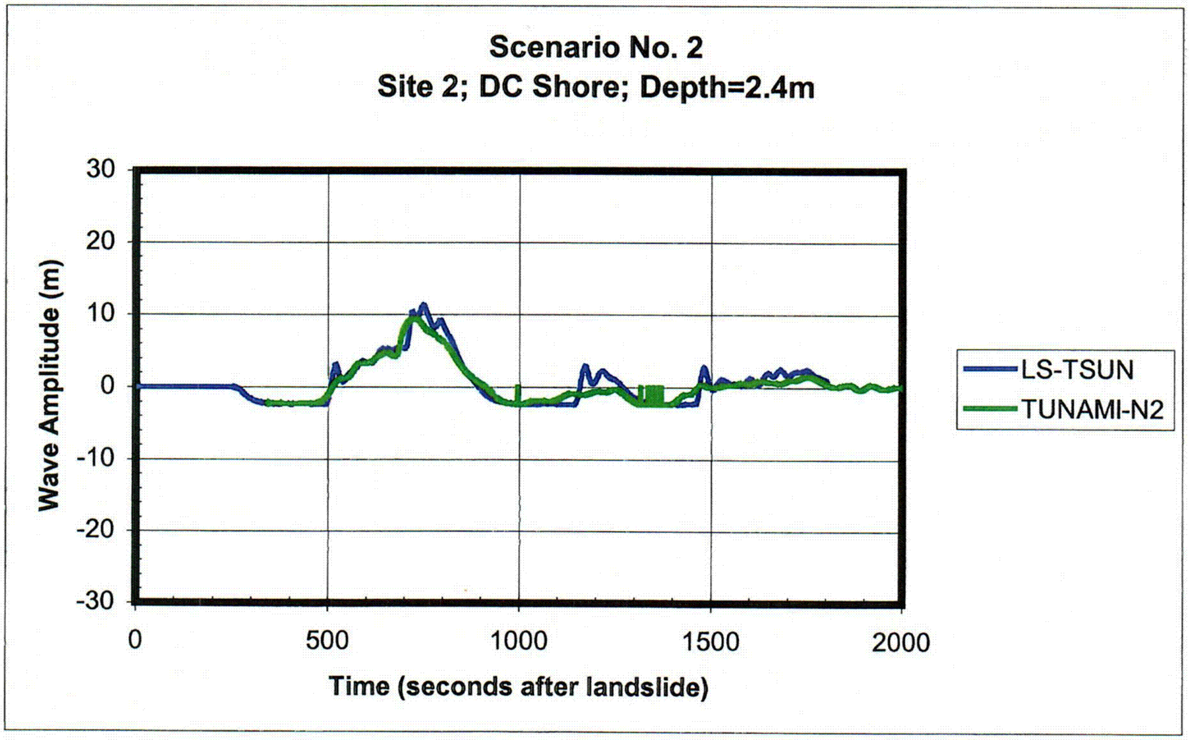

Figure 8 Wave amplitude time histories at Site 1 (above) and Site 2 (below) for Landslide Scenario No. 2.

C09

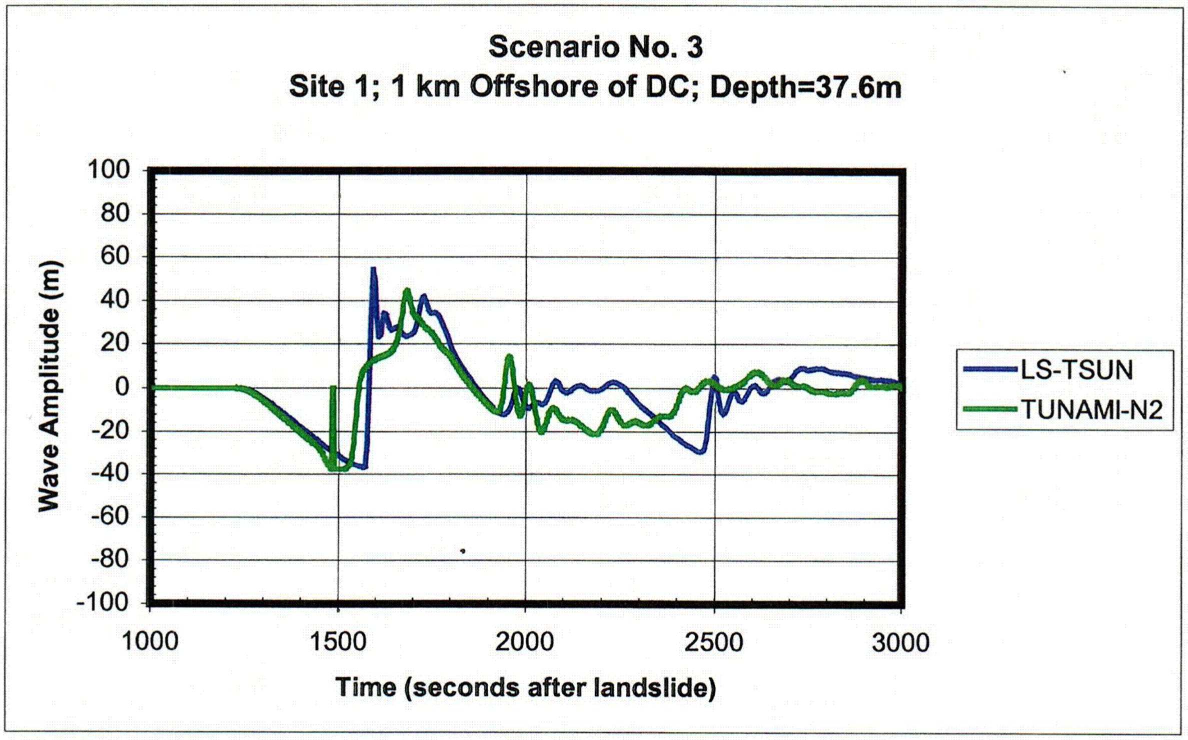

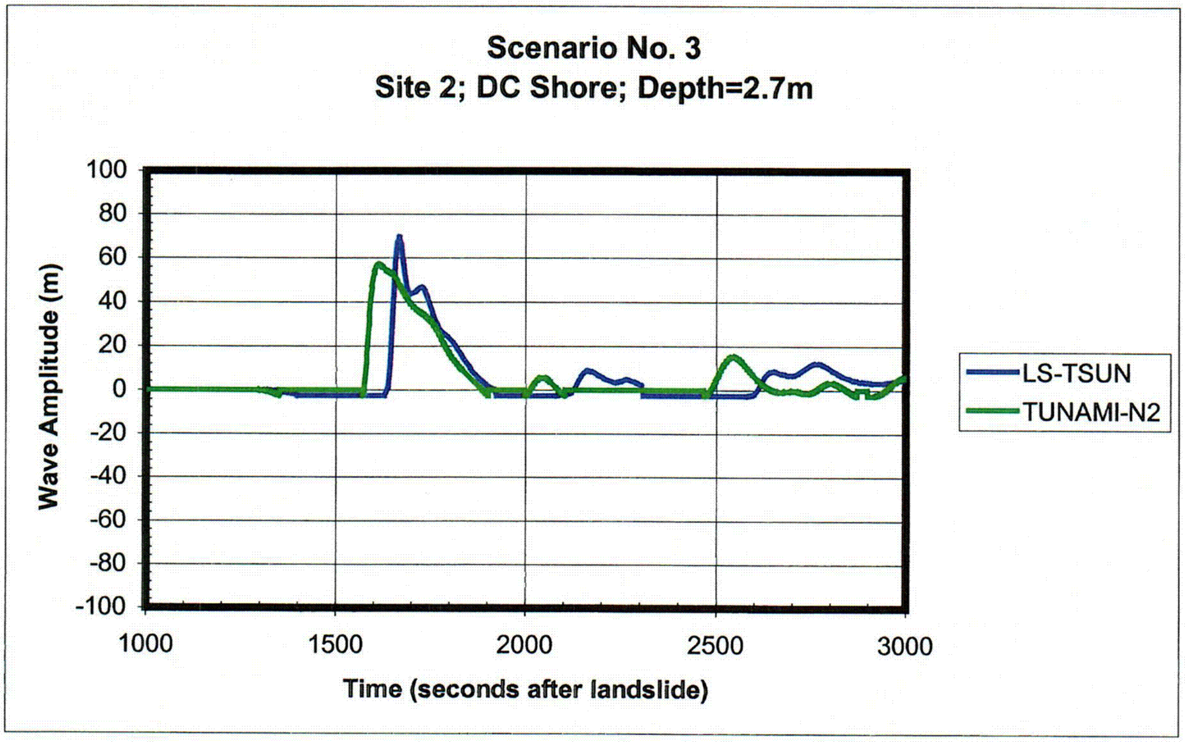

Figure 9 Wave amplitude time histories at Site 1 (above) and Site 2 (below) for Landslide Scenario No. 3.

C10

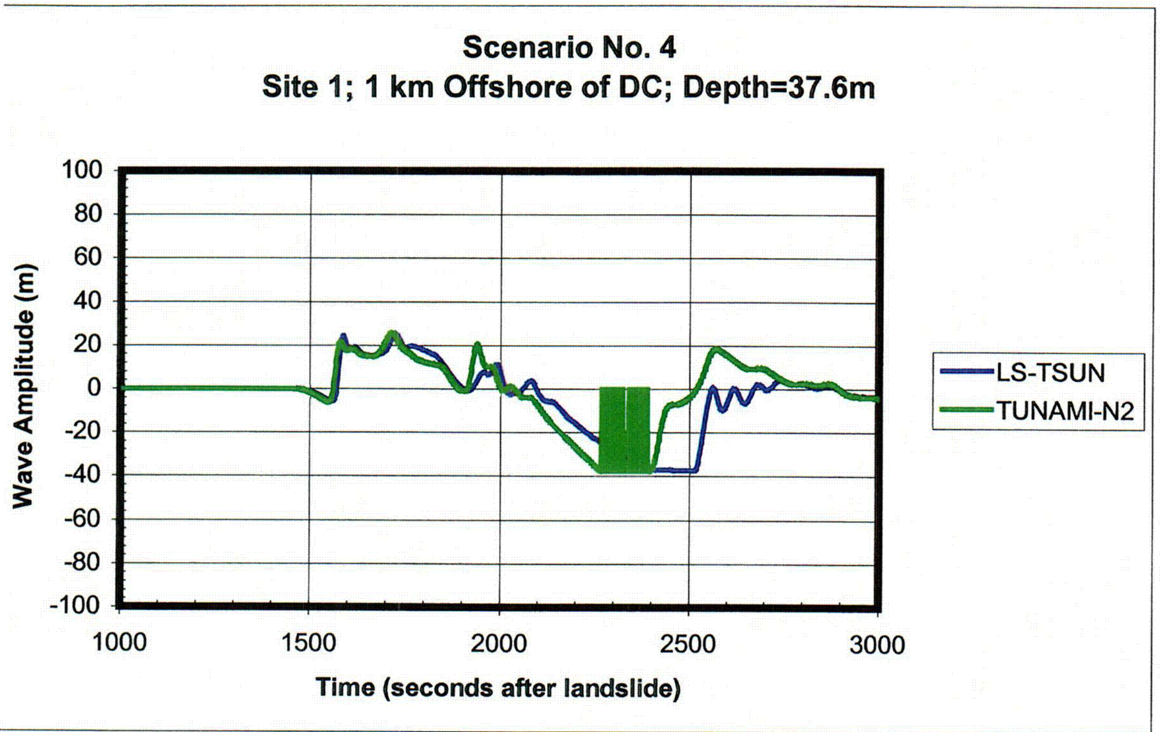

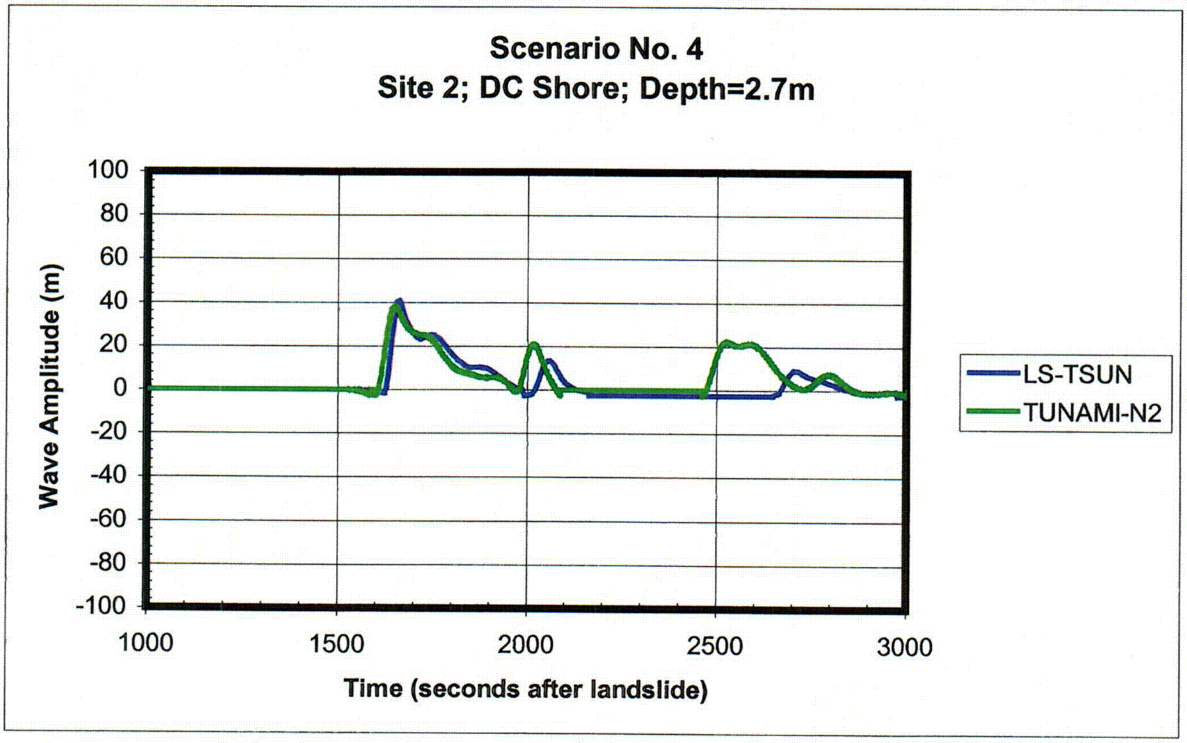

Figure 10 Wave amplitude time histories at Site 1 (above) and Site 2 (below) for Landslide Scenario No. 4.

C11

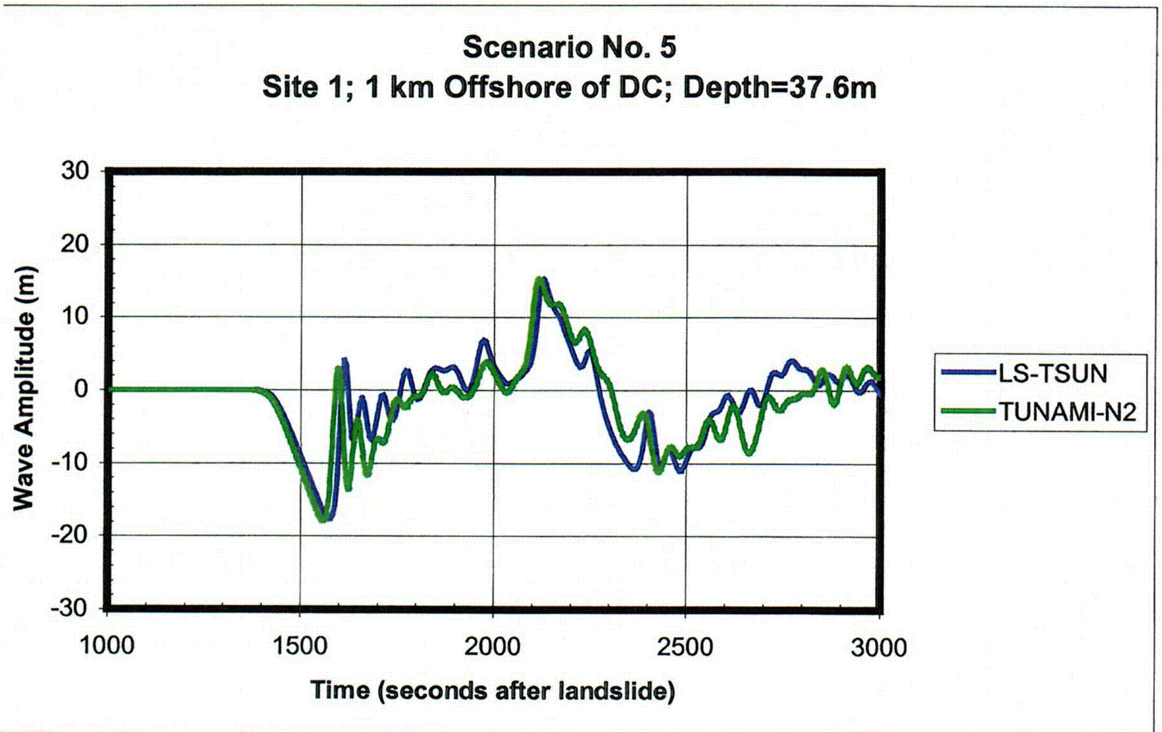

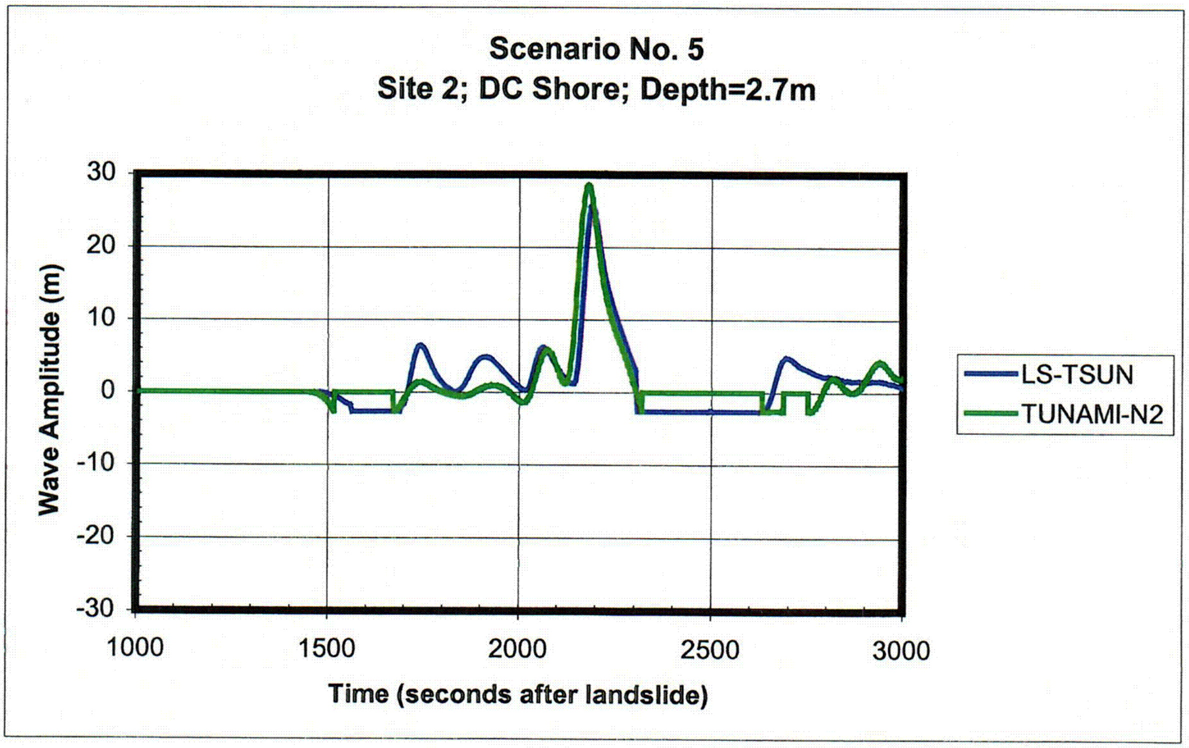

Figure 11 Wave amplitude time histories at Site 1 (above) and Site 2 (below) for Landslide Scenario No. 5.

C12

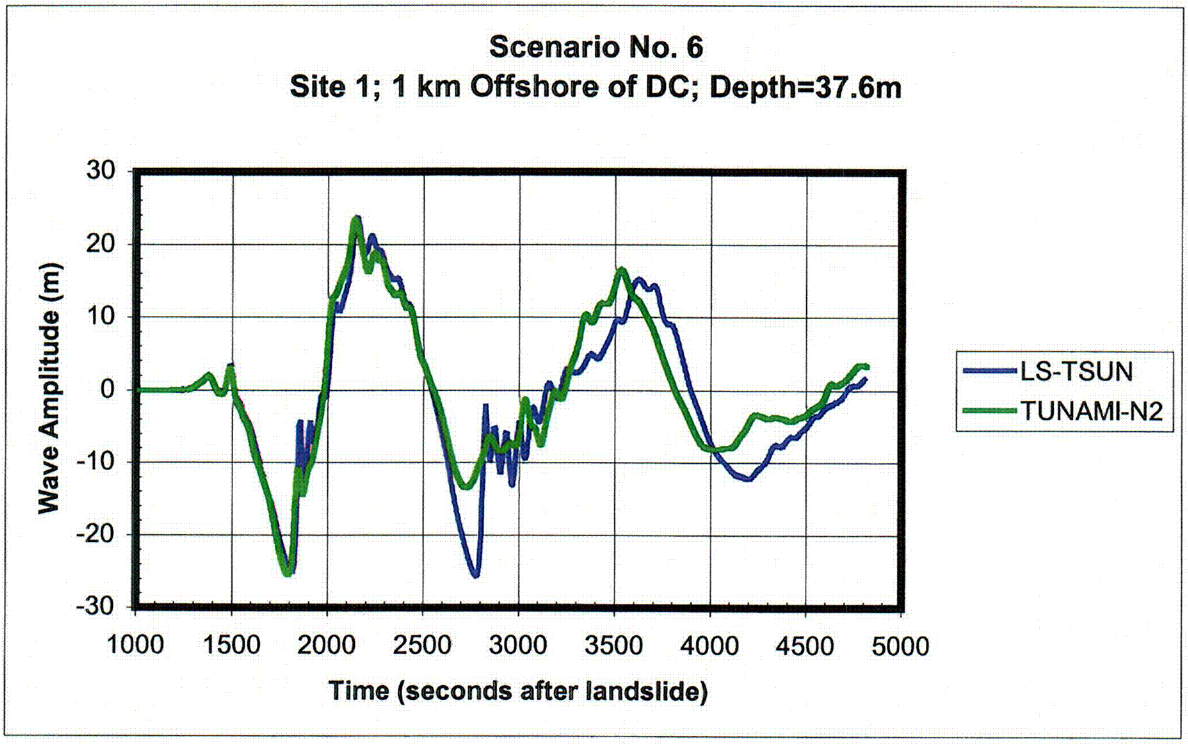

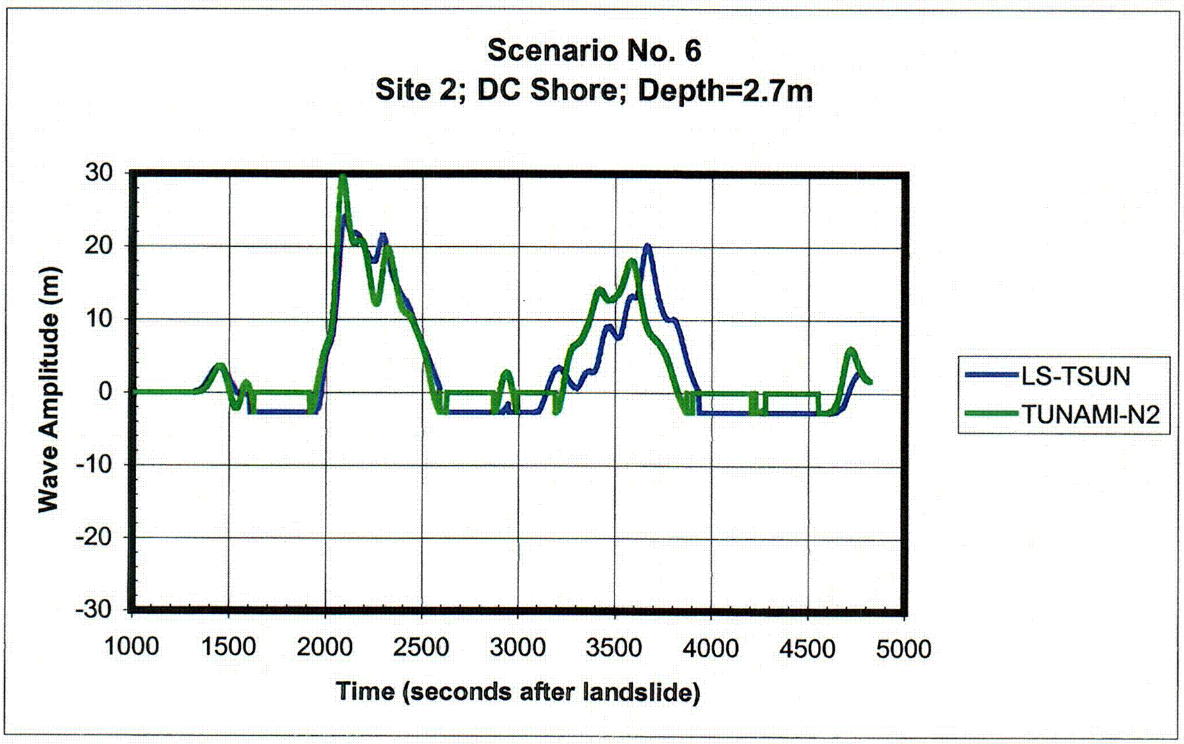

Figure 12 Wave amplitude time histories at Site 1 (above) and Site 2 (below) for Landslide Scenario No. 6.

C13

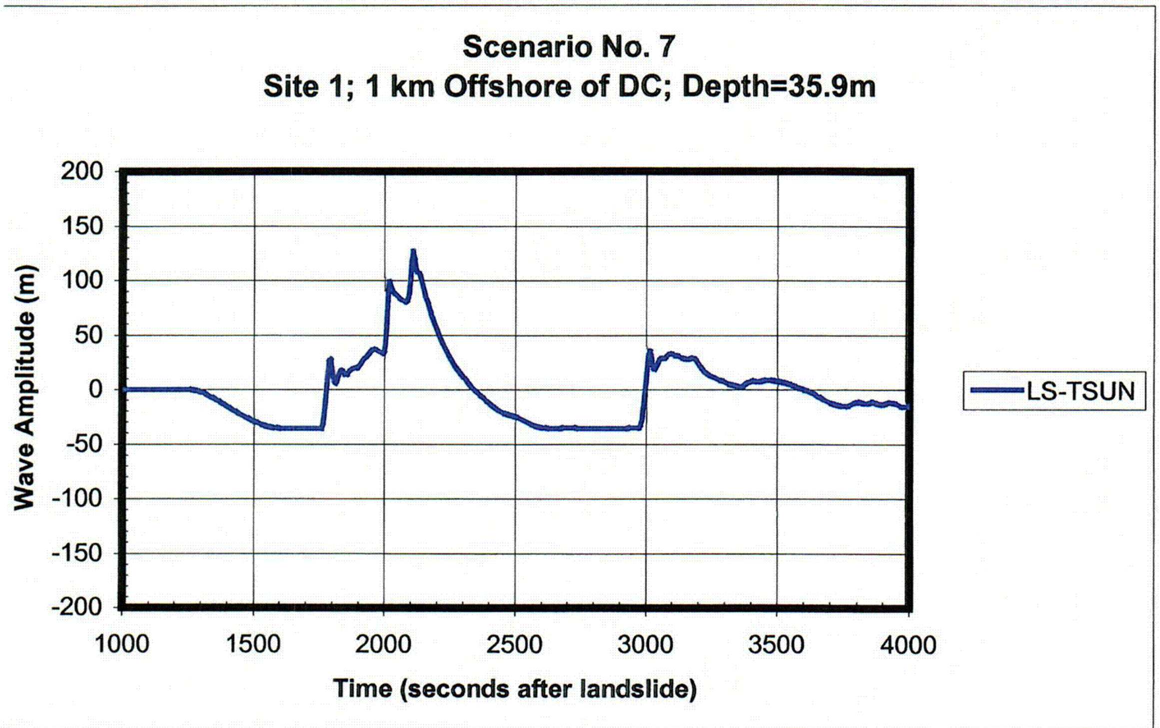

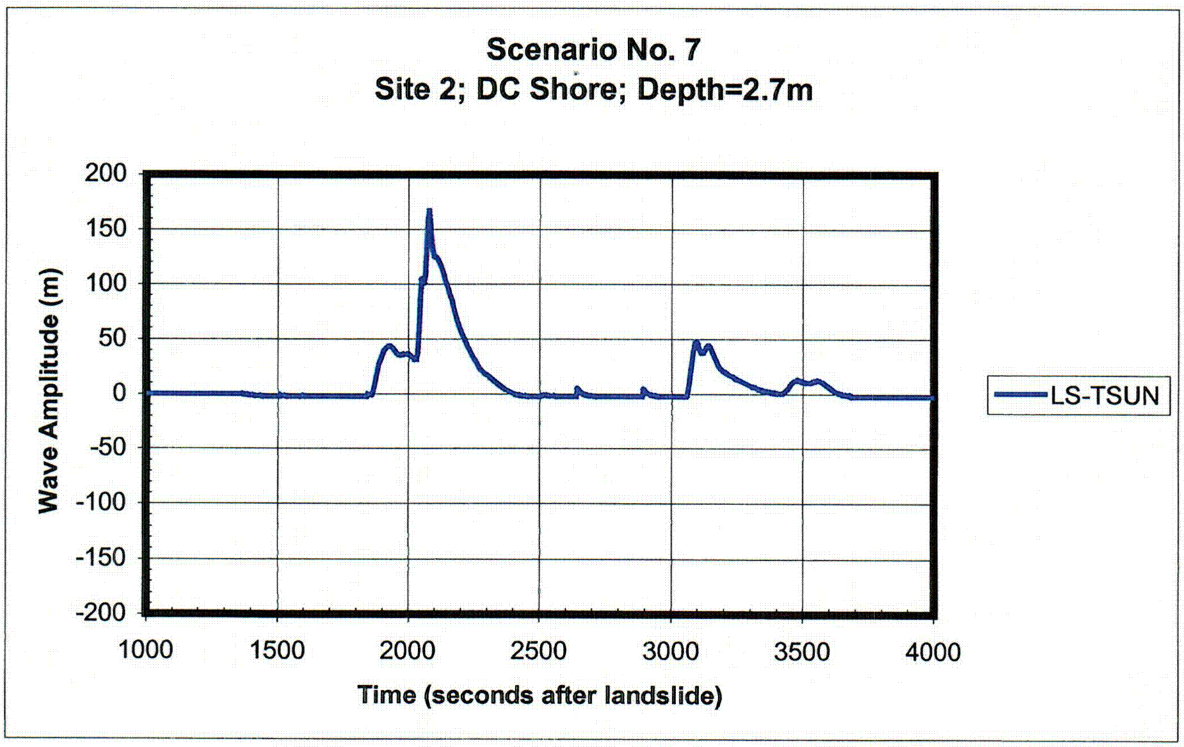

Figure 13 Wave amplitude time histories at Site 1 (above) and Site 2 (below) for Landslide Scenario No. 7.

C14

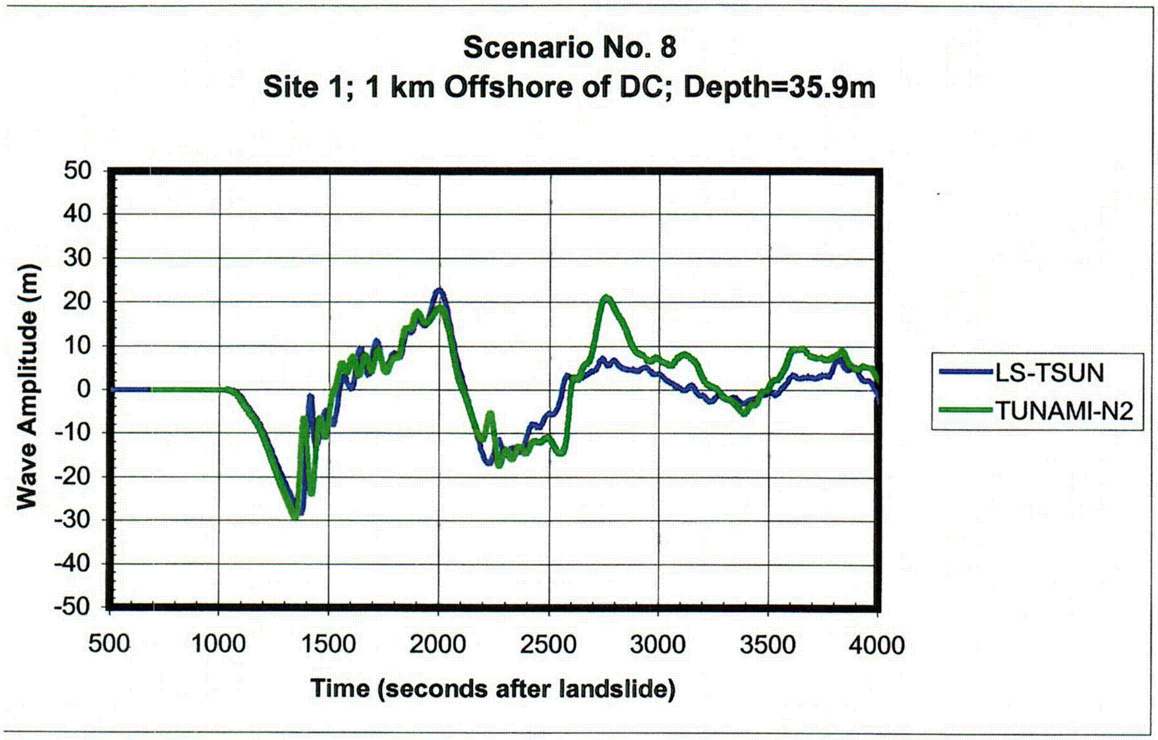

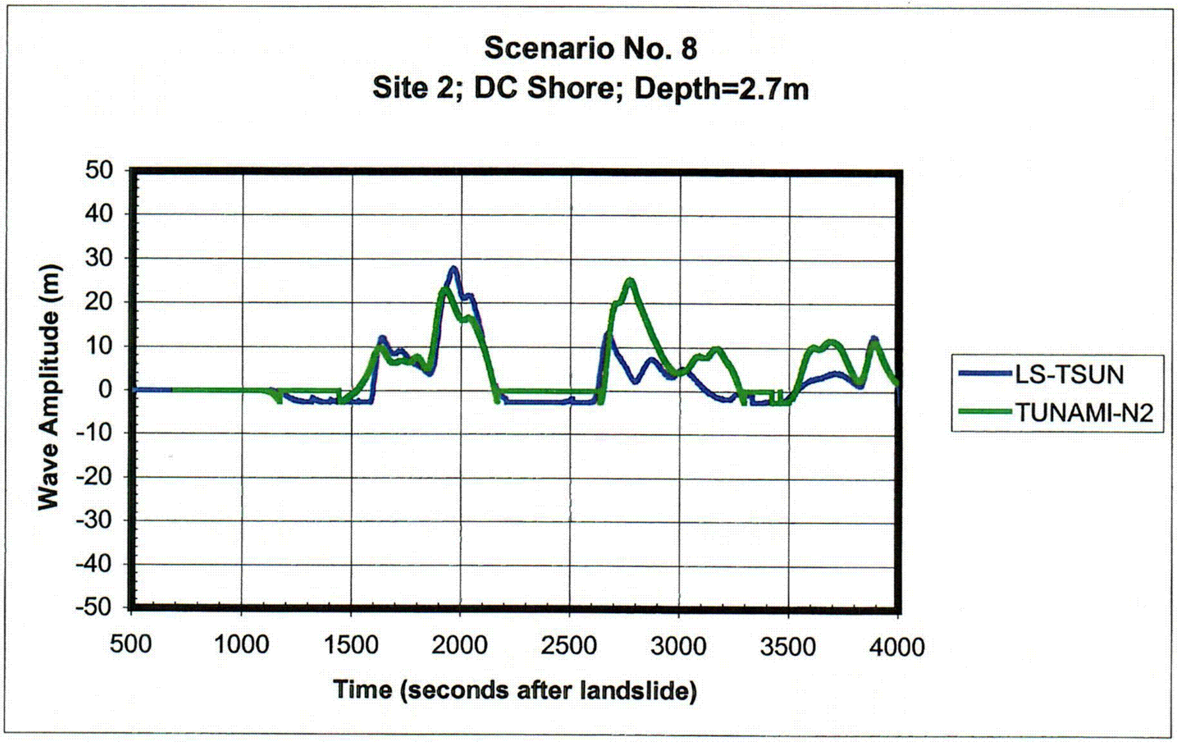

Figure 14 Wave amplitude time histories at Site 1 (above) and Site 2 (below) for Landslide Scenario No. 8.

C15

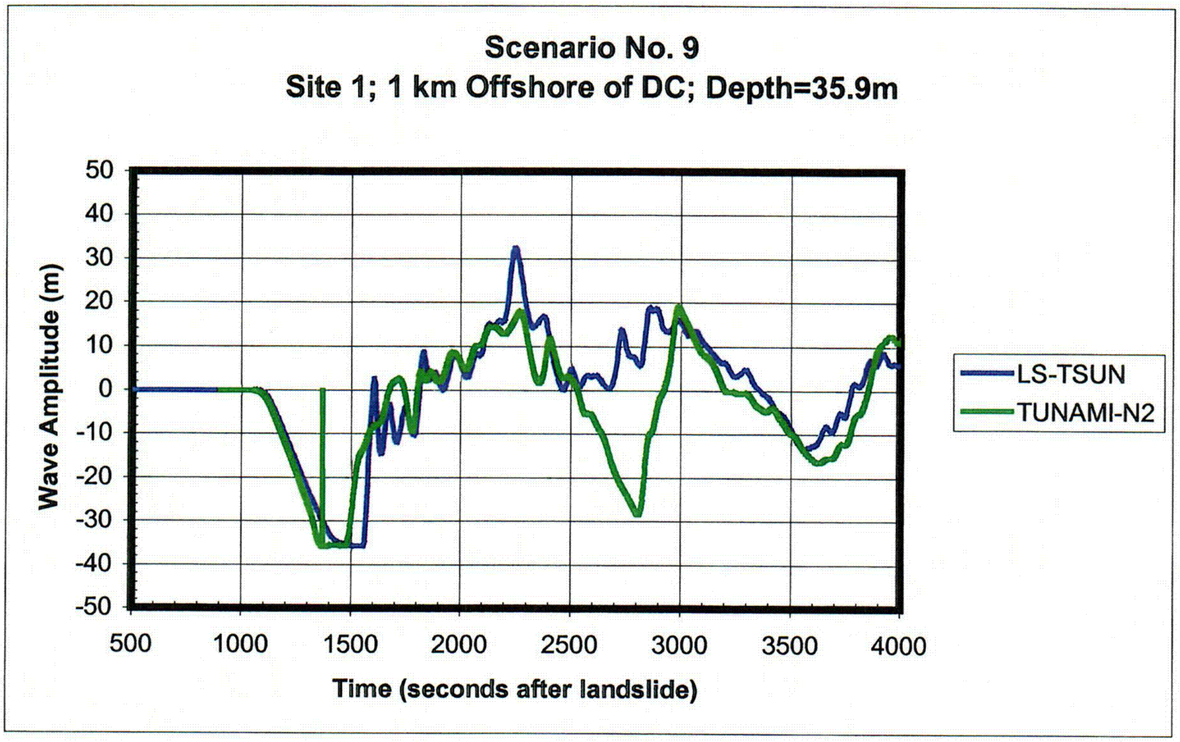

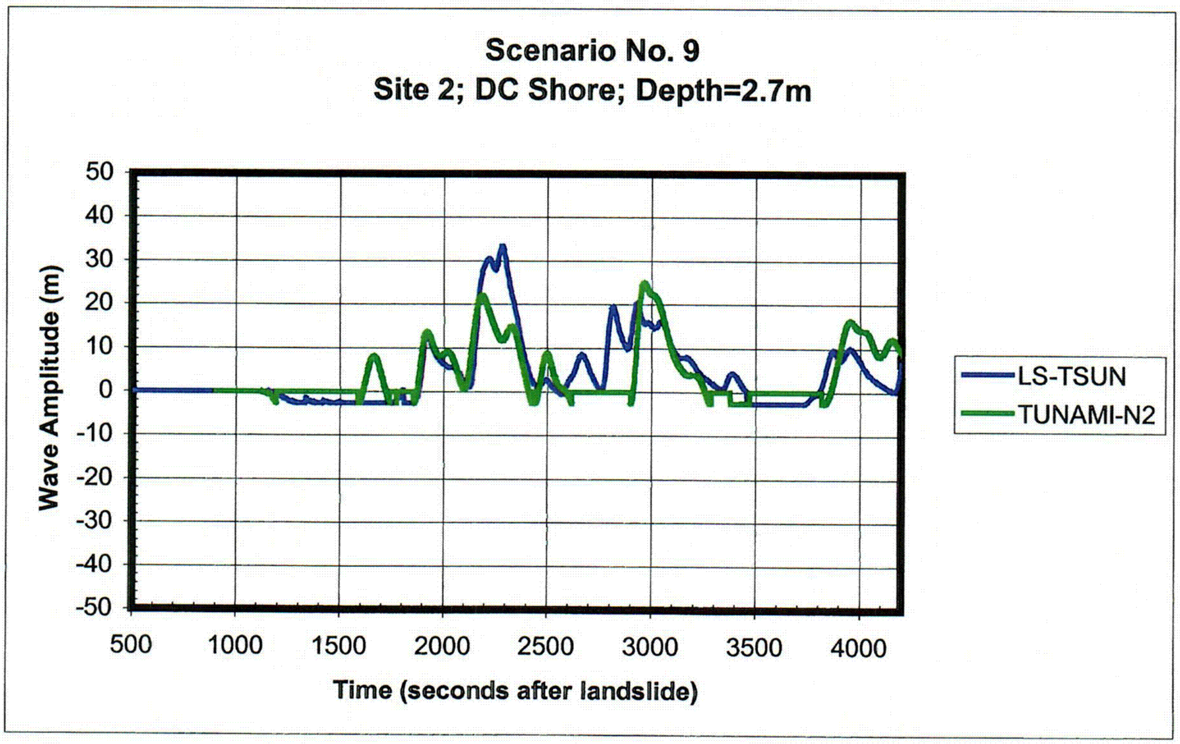

Figure 15 Wave amplitude time histories at Site 1 (above) and Site 2 (below) for Landslide Scenario No. 9.

C16

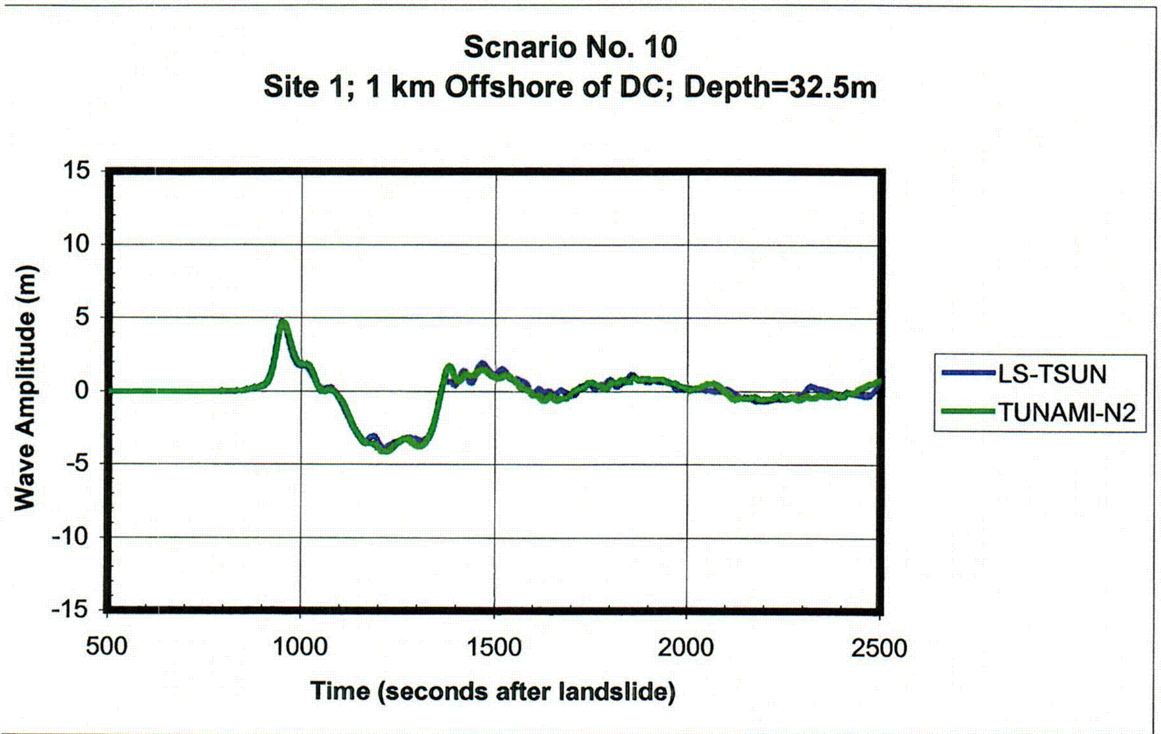

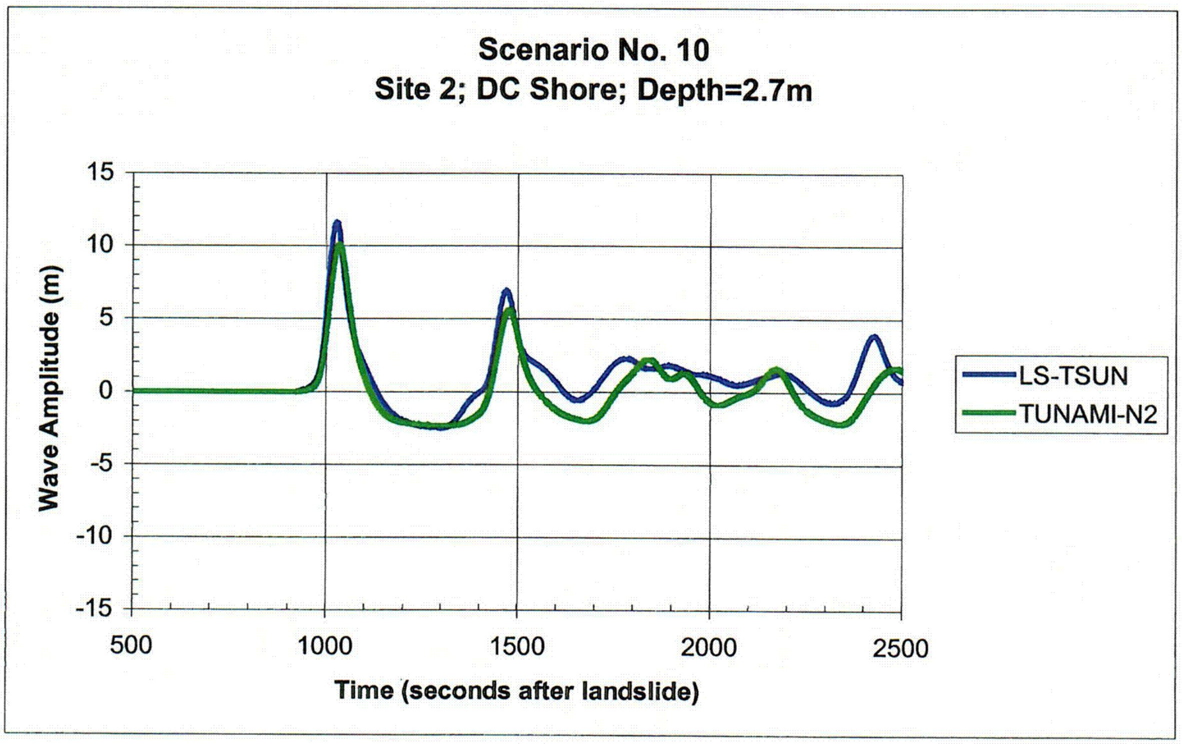

Figure 16 Wave amplitude time histories at Site 1 (above) and Site 2 (below) for Landslide Scenario No. 10.

C17

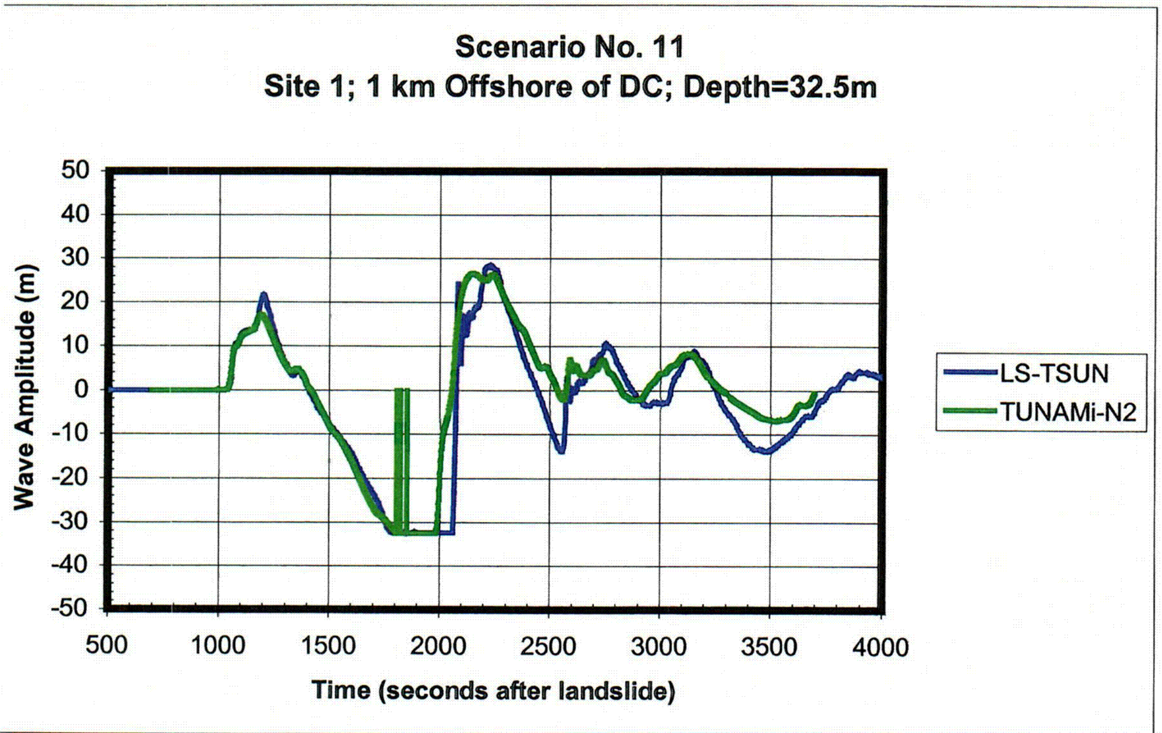

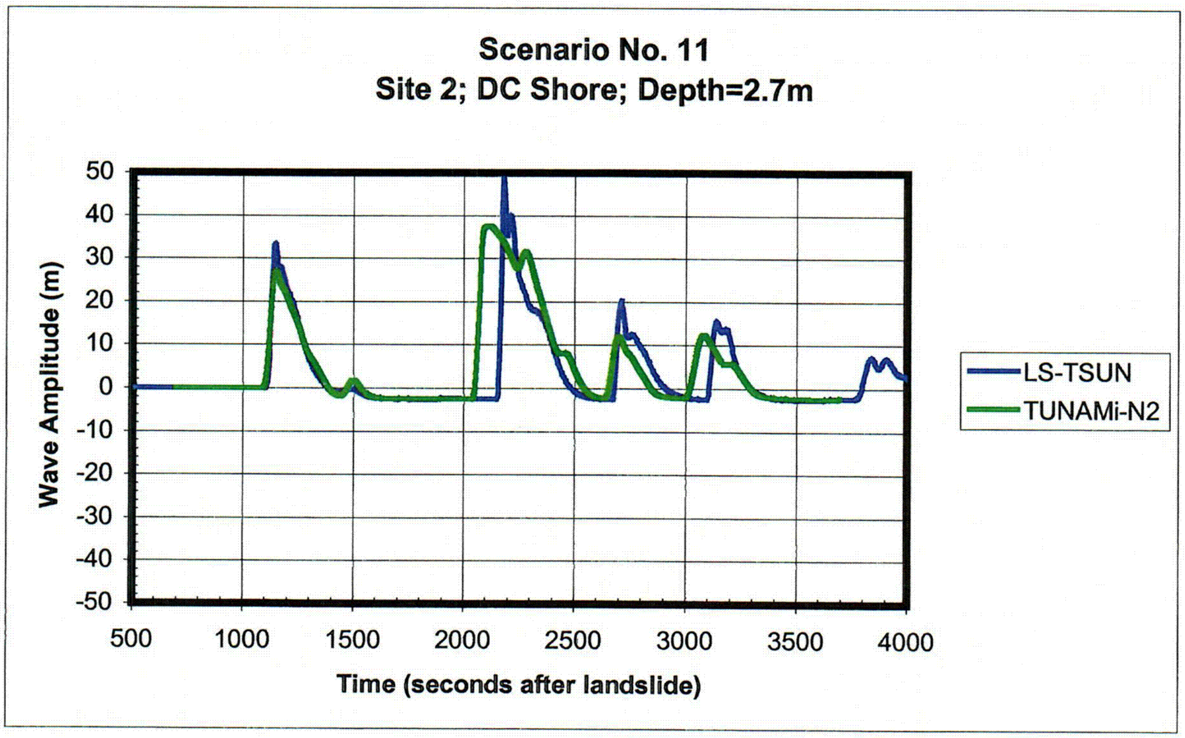

Figure 17 Wave amplitude time histories at Site 1 (above) and Site 2 (below) for Landslide Scenario No. 11.

C18

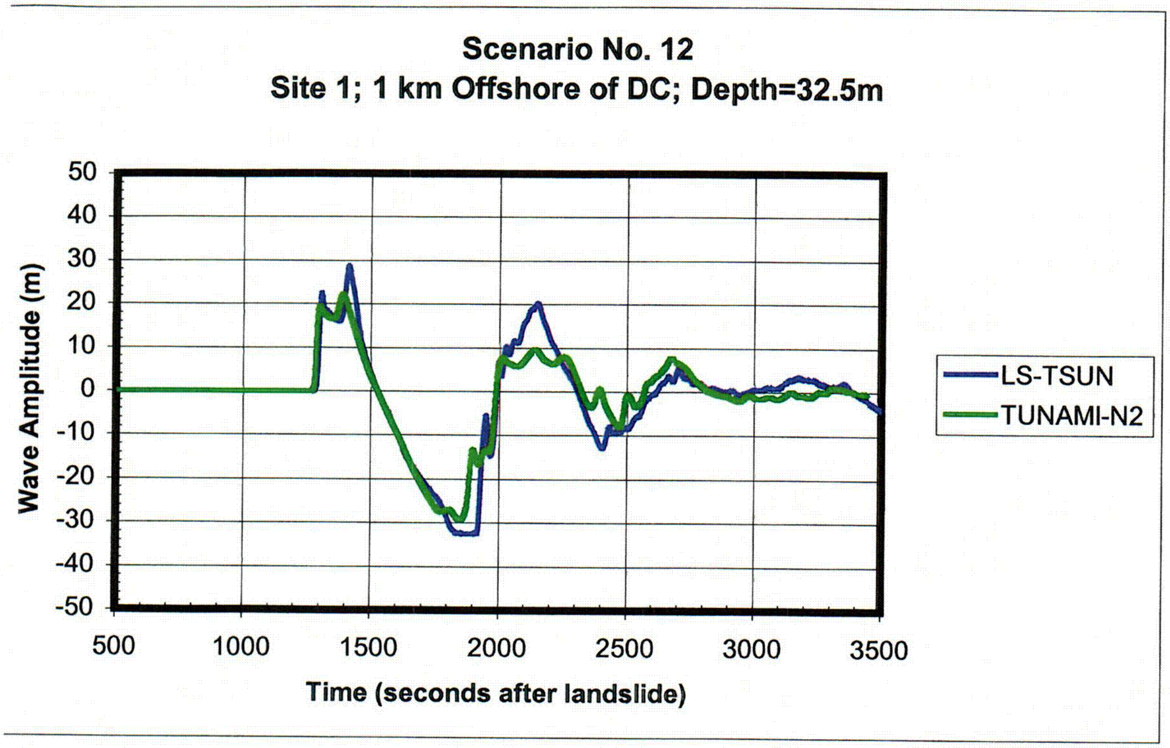

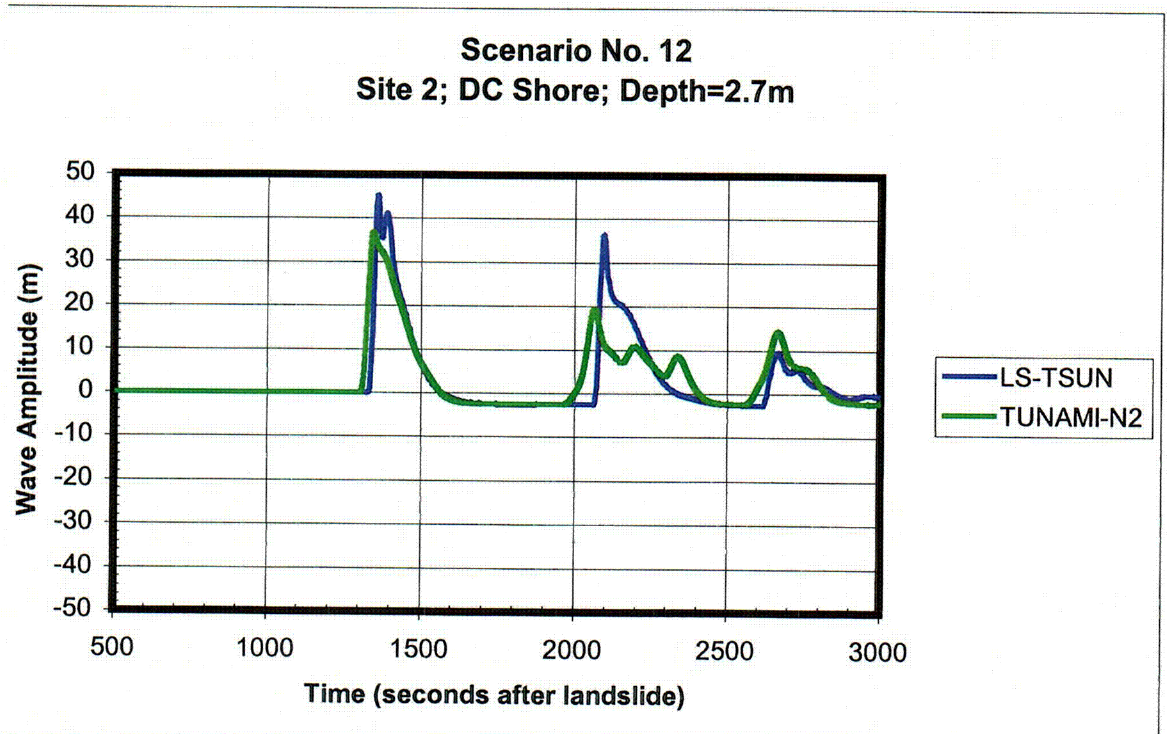

Figure 18 Wave amplitude time histories at Site 1 (above) and Site 2 (below) for Landslide Scenario No. 12.

C19

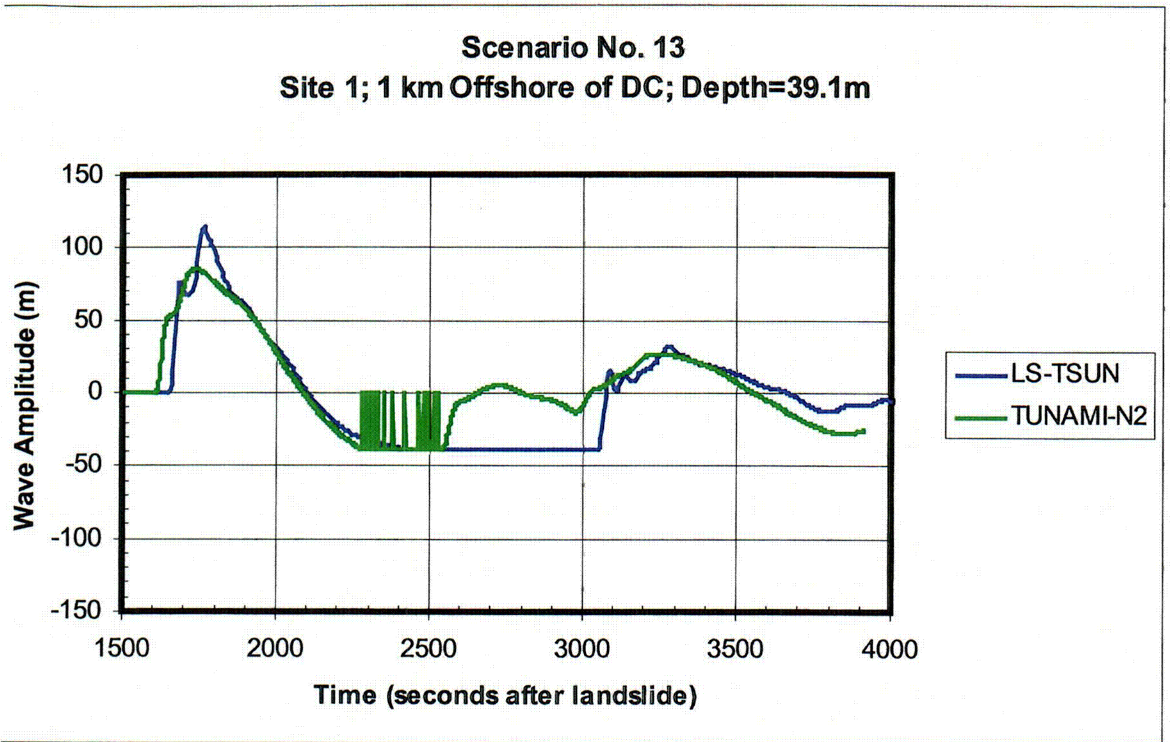

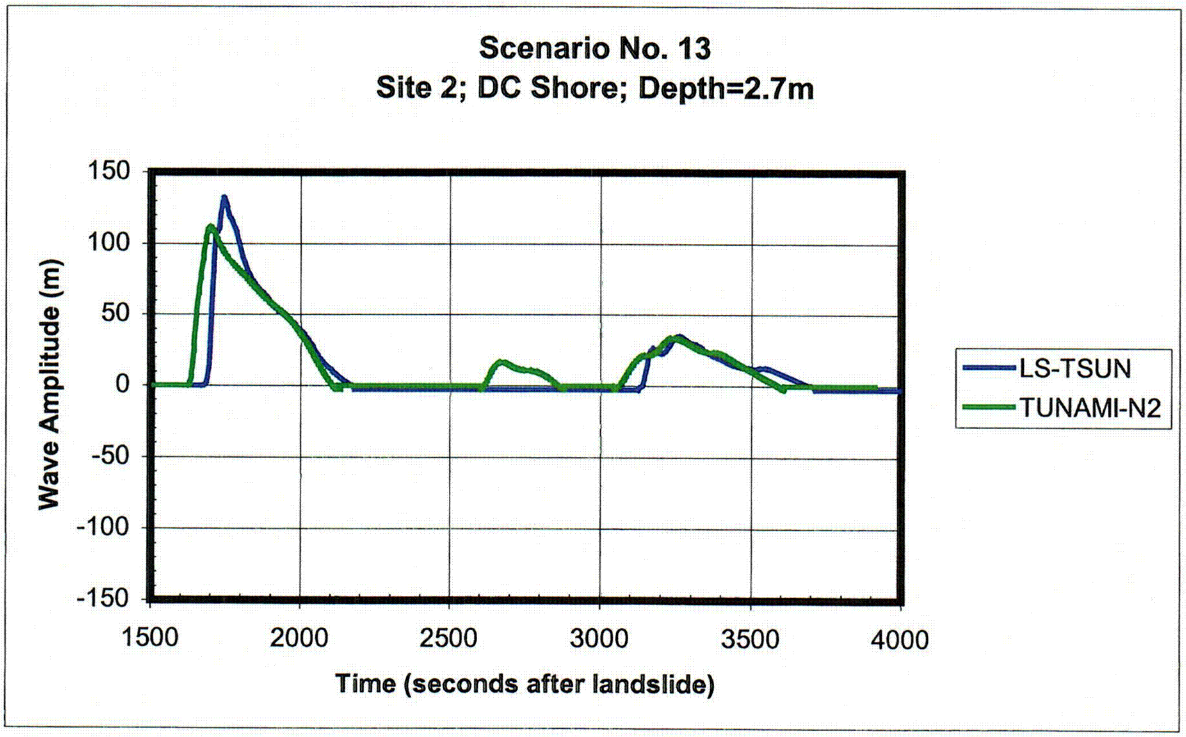

Figure 19 Wave amplitude time histories at Site 1 (above) and Site 2 (below) for Landslide Scenario No. 13.

C20